

國立臺灣大學生命科學院生化科技學系

碩士論文

Department of Biochemical Science and Technology

College of Life Science

National Taiwan University

Master Thesis

從菸草毛狀根之型態與轉錄體探討根毛農桿菌
rol 基因之功能

**Functional exploration of *Agrobacterium rhizogenes*
rol genes by morphological and transcriptomic
analyses of tobacco hairy roots**



林筱涵

Hsiao-Han Lin

指導教授：李昆達 博士

Advisor: Kung-Ta Lee, Ph.D.

中華民國 101 年 7 月

July 2012

國立臺灣大學碩士學位論文
口試委員會審定書

從菸草毛狀根之型態與轉錄體探討根毛農桿菌
rol 基因之功能

**Functional exploration of *Agrobacterium rhizogenes*
rol genes by morphological and transcriptomic
analyses of tobacco hairy roots**

本論文係林筱涵君（ R99B22007 ）在國立臺灣大學生
化科技學系暨研究所完成之碩士學位論文，於民國一百年七
月十九日承下列考試委員審查通過及口試及格，特此證明

口試委員：

李昆達

（簽名）

（指導教授）

劉啟德

鄭秋萍

常曉航

潘子明

楊健志

劉力瑜

系主任、所長

（簽名）

謝誌

四年的時間，一轉眼就過了。感謝 李昆達老師，願意給當年仍升大三的我一個機會，進入發酵實驗室學習。從一開始連滅菌指示膠帶都不認識的我，經過眾多學長姊的教導與鼓勵，有了今天的研究成果。謝謝老師！我由衷感激您。

感謝 劉啟德老師的耐心聆聽、及細心的指導，讓我無論是在試驗設計、實驗過程、或結果分析都能想的更加透徹、仔細。在論文撰寫的過程中，也得到您許多寶貴的意見。謝謝您。

除了上述兩位恩師，在本篇撰寫的過程中，還得到許多人的幫助，分述如下。首先，要感謝 劉力瑜老師慷慨地提供生物統計、R 程式、以及試驗設計的相關諮詢，讓相關數據的生物意義得以彰顯。感謝生科院 TechComm 提供豐富的軟、硬體資源，讓實驗進行順利不少。在論文撰寫初期，要感謝臺大寫作中心 陳巧玲的指導，讓我對於論文寫作有完整的了解與寶貴的學習經驗。還要感謝 鄭秋萍老師、常怡雍老師、以及 楊健志老師對本篇論文提供的意見與指教，讓本篇論文更加完備。感謝各位老師的教導，筱涵由衷感激。

在研究的過程中，我要特別感謝不辭勞苦分擔菸草種植、毛狀根繼代、以及算根長的大中；以及無論是在試驗設計、文獻探討、結果分析及討論都讓我獲益良多的的榮顯。除了上述兩位，我也要感謝發酵實驗室的大家：派派、小宏、阿蘇、松輝、以則、獻仁、大仔、舒晴、鏡介、子耕、小畢、念杰、威霆...。離開後，我必然想念那些與各位一起度過的美好日子。我想念那些吃飯兼散步的悠閒時光，那些在植物室待到天荒地老都繼代不完的無奈時光，那些要討論實驗卻不知不覺聊起天來的莫名時光，那些在上臺報告前三天的焦慮時光，那些在抽 RNA 時大家都退避三舍的驚恐時光，那些直到半夜學生卻不准我們下班的苦命應徵助教時光...。因為有你們，在發酵實驗室的日子顯得如此多采多姿。謝謝你們！

最後，要感謝我的家人們。感謝你們從小到大的呵護、栽培、教導、與陪伴。因為有你們，才有今日的我。

筱涵謹誌於

國立臺灣大學生化科技學系暨研究所

中華民國一零一年七月

摘要

毛狀根 (hairy root) 是根毛農桿菌 (*Agrobacterium rhizogenes*) 感染植物後誘發生成的癌化組織，此組織被視為是最有潛力的植物次級代謝物生產工廠。文獻指出根毛農桿菌 Ri 質體上的 *rol* 基因群 (*rolA* 、 *rolB* 、 *rolC* 以及 *rolD*) 會影響毛狀根的生成。然而，尚未有文獻報導 *rol* 基因群如何影響毛狀根形態，以及這些基因影響的植物生理機能。因此，本研究利用根毛農桿菌野生型及 *rol* 基因缺陷株感染菸草，分析所生成的毛狀根在形態以及轉錄體學之差別。形態調查結果顯示，*rolB/rolC* 根毛農桿菌缺陷株在毛狀根誘導率及外表型上與野生型有顯著差異，而 *rolA/rolD* 的影響不大。轉錄體分析 *rolB/rolC* 缺陷毛狀根與野生型毛狀根的結果顯示：RolB 蛋白質可能對於菸草毛狀根的脂質運送、細胞胺基酸相關生合成路徑、創傷反應、以及乙烯刺激反應具有正向調控功能；RolC 蛋白質則對於創傷反應、化學刺激反應、醣類代謝、以及脂質運送具有正向調控功能。上述結果揭示了 *rolB/rolC* 如何影響毛狀根形態，以及它們在毛狀根組織中所參與的生理機能。

關鍵字：毛狀根、*rol* 基因群、根毛農桿菌、菸草、轉錄體分析

Abstract

Hairy root is the tumorized tissue induced when *Agrobacterium rhizogenes* infects plants, and is considered as the most powerful plant secondary metabolites-producing system. The formation of hairy root have been known to related to four root inducing (*rol*) genes *rolA*, *rolB*, *rolC*, and *rolD* that lie in the transferred DNA (T-DNA) of *A. rhizogenes* root inducing (Ri) plasmid. However, no studies showed how these *rol* genes affect hairy root architecture. Also, there is no comprehensive –omics information of how plant cell is manipulated by the *rol* genes. Therefore, this study tried to answer these questions by morphological and transcriptomic analysis of tobacco hairy root induced by wild type and *rol* deletion mutant of *A. rhizogenes*. Morphological analysis revealed that lacking *rolB* and *rolC* cause impaired hairy root syndrome, while lacking *rolA* and *rolD* had little or no effects. Transcriptomic comparison of *rolB* / *rolC* deleted hairy roots compared with that of wild type indicate that RolB may positively regulate lipid transport, cellular amino acid derivative biosynthesis process, response to wounding, and response to ethylene stimulus. Meanwhile, the biological processes that may be positively regulated by RolC are response to wounding, response to chemical stimulus, carbohydrate metabolic process, and lipid transport. The results revealed how *rolB* and *rolC* affect hairy root morphology and what are the corresponding biological processes they manipulated.

Keywords: hairy root, *rol* genes, *A. rhizogenes*, *N. tabacum*, transcriptomic analysis

Abbreviations

MS medium	Murashige and Skoog medium
½ MS+Ce	Half strength MS medium supplied with 300 ppm cefotaxime
W38	<i>N. tabacum</i> L. cv. Wisconsin 38
WTA4	Wild type <i>A. rhizogenes</i> strain A4
$\Delta rolA$	<i>rolA</i> deleted <i>A. rhizogenes</i> strain A4
$\Delta rolB$	<i>rolB</i> deleted <i>A. rhizogenes</i> strain A4
$\Delta rolC$	<i>rolC</i> deleted <i>A. rhizogenes</i> strain A4
$\Delta rolD$	<i>rolD</i> deleted <i>A. rhizogenes</i> strain A4
HR WT	Hairy root induced by wild type <i>A. rhizogenes</i> strain A4
HR $\Delta rolA$	Hairy root induced by <i>rolA</i> deleted <i>A. rhizogenes</i> strain A4
HR $\Delta rolB$	Hairy root induced by <i>rolB</i> deleted <i>A. rhizogenes</i> strain A4
HR $\Delta rolC$	Hairy root induced by <i>rolC</i> deleted <i>A. rhizogenes</i> strain A4
HR $\Delta rolD$	Hairy root induced by <i>rolD</i> deleted <i>A. rhizogenes</i> strain A4
DPI	Days post infection
DREPI	Days of the first root emergence post infection
RL ratio	The primary hairy root number per leaf disc
MRL	Main root length
BRN	Branch root number
TBRL	Total branch root length
BRD	Branch root density (cm ⁻¹)
GO	Gene ontology
qRT-PCR	Quantitative real time-polymerase chain reaction

Contents

口試委員會審定書	i
謝誌	ii
摘要	iii
Abstract.....	iv
Chapter 1. Introduction	5
1.1 Aim of research	5
1.2 General backgrounds of hairy root.....	5
1.3 RolA	8
1.4 RolB	10
1.5 RolC	12
1.6 RolD	14
1.7 Research strategies	15
Chapter 2. Materials and Methods	17
2.1 Plant materials and growth conditions	17
2.2 Bacteria and growth conditions.....	17
2.3 Genotype confirmation for <i>A. rhizogenes</i> strain A4 derivatives.....	18
2.4 Hairy root induction	18
2.5 Hairy root initiation test	19
2.6 Hairy root genotype confirmation.....	20
2.7 Analysis of hairy root architectures	20
2.8 Statistical analysis	21
2.9 RNA extraction	22
2.10 Microarray labeling, scanning, and data extracting	23
2.11 Gene ontology of microarray data.....	23
2.12 qRT-PCR.....	24

Chapter 3. Results	26
3.1 Genotype confirmation of <i>rol</i> gene-deficient <i>A. rhizogenes</i> strain A4	26
3.2 Tobacco infection by <i>A. rhizogenes</i> strain A4 and its derivatives	26
3.3 Confirmation of hairy root genotype.....	27
3.4 Hairy root initiation test	28
3.5 Measurements of hairy root architecture.....	29
3.6 Microarray Data Analysis	32
3.7 Gene ontology of HR D <i>rolB</i> down-regulated genes	33
3.8 Gene Ontology of HR D <i>rolC</i> down-regulated genes	33
3.9 qRT-PCR Analysis of the Gene Ontology-extracted genes	34
Chapter 4. Discussions	36
4.1 <i>rolB</i> and <i>rolC</i> play crucial roles in hairy root initiation.....	36
4.2 <i>rolB</i> and <i>rolC</i> affect hairy root architecture more drastically	36
4.3 Difficult maintenance of the HR D <i>rolB</i> and HR D <i>rolC</i> clones.....	37
4.4 Comparison between the microarray and qRT-PCR analyses	38
4.5 Biological processes manipulated in the absence of <i>rolB</i>	38
4.6 Biological processes manipulated in the absence of <i>rolC</i>	40
4.7 Deduced biological functions of <i>rolB</i>	41
4.8 Deduced biological functions of <i>rolC</i>	42
Chapter 5. Conclusion	44
Tables.....	45
Figures	63
References	84
Appendix	91

List of Figures

Figure 1-1. Hairy root.....	63
Figure 1-2. <i>A. rhizogenes</i> under microscope.....	64
Figure 1-3. Molecular mechanisms of how <i>A. rhizogenes</i> infects plant cell.....	65
Figure 1-4. The TL-DNA region of <i>A. rhizogenes</i> strain A4.....	66
Figure 2-1. Target region of the pK18HRrol check primers.....	67
Figure 2-2. Measuring hairy root architecture.....	68
Figure 2-3. Explanation of Gene Ontology diagram.....	69
Figure 3-1. Genotype confirmation of <i>A. rhizogenes</i> strain A4 and its derivatives.....	70
Figure 3-2. Growth curve of wild type and the <i>rol</i> gene-deficient <i>A. rhizogenes</i> strain A4.....	71
Figure 3-3. Confirmation of hairy root genotype.....	72
Figure 3-4. Phenotypes of <i>A. rhizogenes</i> A4 and its derivatives-infected tobacco leaf discs at 21 dpi.....	73
Figure 3-5. Days to the first root emergence post induction (DREPI).....	74
Figure 3-6. Primary root number per leaf disc (RL ratio) at 21 dpi.....	75
Figure 3-7. Selected hairy root appearances after 18 days post sub-culturing.....	76
Figure 3-8. Main root length of <i>A. rhizogenes</i> A4 and its <i>rol</i> gene-deficient derivatives.....	77
Figure 3-9. Branch root number of <i>A. rhizogenes</i> A4 and its <i>rol</i> gene-deficient derivatives.....	78
Figure 3-10. Total branch root length of <i>A. rhizogenes</i> A4 and its <i>rol</i> gene-deficient derivatives.....	79
Figure 3-11. Branch root density of <i>A. rhizogenes</i> A4 and its <i>rol</i> gene-deficient derivatives.....	80
Figure 3-12. The constitutive expressed gene under 2-fold cut off.....	81
Figure 3-13. Gene ontology of HR $\Delta rolB$ down-regulated genes.....	82
Figure 3-14. Gene ontology of HR $\Delta rolC$ down-regulated genes.....	83

List of Tables

Table 2-1. Primers used for genotype confirmation.....	45
Table 2-2. Primers used for qRT-PCR test.....	46
Table 3-1. Numbers of differentially expressed genes analyzed by microarray.	49
Table 3-2. GO term of down regulated genes in HR $\Delta rolB$ compared to HR WT.....	50
Table 3-3. GO analysis in terms of biological process of HR $\Delta rolB$ down regulated genes compared with those in HR WT.....	51
Table 3-4. GO results of HR $\Delta rolC$ down regulated genes compared to HR WT.....	56
Table 3-5. GO analysis in terms of biological process of HR $\Delta rolC$ down regulated genes compared with those in HR WT.....	57



Chapter 1. Introduction

1.1 Aim of research

Hairy root is considered as the most powerful plant secondary metabolites-producing system because of its hormone-free culturing ability, high-level secondary metabolites production, and short-term biomass accumulation (Bulgakov, 2008; Ono and Tian, 2011; Banerjee et al., 2012). The formation of hairy root have been known to be related to four root inducing (*rol*) genes *rolA*, *rolB*, *rolC*, and *rolD* that lie in the transferred DNA (T-DNA) of *Agrobacterium rhizogenes* (Bulgakov, 2008; Welandar and Zhu, 2010). However, the biological functions of *rolA*, *rolB*, and *rolC* remains unclear to date, despite that they had been discovered since 1985 (White et al., 1985) and that many papers aimed to uncover their biological functions (Estruch et al., 1991; Estruch et al., 1991; Filippini et al., 1996). In order to unveil the biological functions *rol* genes have in hairy root, we aimed to understand the biological process changed in the absence of single *rol* genes in a comprehensive way. We hope this will shed light on the *rol* genes' biological function research and / or improve hairy root plant secondary metabolite producing system. Therefore, this study used microarray technology to comprehensively analysis the biological process changes in the presence / absence of single *rol* genes.

1.2 General backgrounds of hairy root

Hairy root (Fig. 1-1b, c, and d) is an ectopic plant tissue emerged after *Agrobacterium rhizogenes* (Fig. 1-2) infecting plant (Fig. 1-1a). It was first known as a plant disease in apple trees in the 1930s (Riker et al., 1930). Thereafter, hairy root has also been found in many dicot plants, but not in the monocots, and is viewed as a plant

disease (Ark and Thompson, 1961). In the 1980s, two unique characters of hairy root system were discovered. First, it can grow in the absence of exogenous phytohormones (Spano et al., 1981). Second, plant secondary metabolites were observed to be accumulated in high levels in the ectopic root tissue of *Beta vulgaris* and *Nicotiana rustica*, respectively (Hamill et al., 1986). In addition to these two unique characters, the fast growing, easy transforming, and long-term stability in transgenic lines make it a perfect system for producing valuable plant secondary metabolites (Toivonen, 1993; Bulgakov, 2008; Ono and Tian, 2011). Therefore, hairy root system is not only referred to as a plant disease, but also as a promising plant factory that produces massive valuable secondary metabolites.

There have been many successful cases of using hairy root system as a plant secondary metabolites factory. For example, the production of resveratrol, an anti-carcinogen compound, was increased more than 100-fold in grape (*Vitis amurensis* Rupr.) hairy root than in normal culture (Kiselev et al., 2007). Another well-established example is the anti-apoptosis compound, ginsenoside, produced by ginseng. By using the hairy root system, the yield of ginsenoside was three times more than that of normal ginseng (Bulgakov et al., 1998). Taxol is a famous anti-cancer compound, produced from pacific yew tree (*Taxus brevifolia*). By using Hairy root system, the production of taxol was 210-fold more than that of normal yew tree (Furmanowa and Syklowska-Baranek, 2000; Kim et al., 2009). Recently, hairy root system has also been used in producing valuable recombinant proteins. Human secreted alkaline phosphatase (Gaume et al., 2003), mucosal adjuvant Ricin B (Gaume et al., 2003), and liver enzyme mammalian P450 2E1 protein (Banerjee et al., 2002) are some of the examples. Thus, hairy root system is a powerful factory not only of plant secondary metabolites but also of valuable recombinant proteins.

Molecules responsible for hairy root emergence after *A. rhizogenes* infection were studied in the 1980s. In 1980, White and Nester showed that the virulent trait of *A. rhizogenes* lie in its large plasmids rather than its chromosome. The plasmids were denoted pRi for their root inducing capacity (White and Nester, 1980) (Fig. 1-3). Further studies showed that fragments of DNA designate transferred DNA (T-DNA) in the large plasmid are responsible for the ectopic hairy root phenotype (White et al., 1982) (Fig. 1-3 green bar). During *A. rhizogenes* infection, the T-DNAs are delivered into plant nucleus and integrated into its chromosome (Slightom et al., 1985) (Fig. 1-3 green bar in the gray circle). After the infection, the genes on the T-DNAs start to function in the infected plant cell (White and Nester, 1980; White et al., 1985). These plant cell-expressed T-DNA genes turn the transformed plant cell into ectopic root (Taylor et al., 1985). The T-DNA harboring root tissue is capable of regeneration into a whole plant when external phytohormones were added (Ooms et al., 1986). The plant regenerated from T-DNA transformed hairy root is termed regenerated plant.

The most commonly studied strain of *A. rhizogenes* is strain A4. It has two T-DNAs designated as T_L-DNA and T_R-DNA (Huffman et al., 1984; Taylor et al., 1985) (Fig. 1-3 the two green bars on Ri plasmid). During infection, the two T-DNAs insert into plant chromosomes independently (Vilaine and Cassedelbart, 1987). Studies showed that both T-DNA regions are able to transform plant cell into hairy root separately, but they work more efficient when both exist (White et al., 1985; Vilaine and Cassedelbart, 1987). T_R-DNA is known to share homologous with tumor-inducing plasmid (pTi) of *Agrobacterium tumefaciens* (White et al., 1985). Thus, the molecular mechanism of how it manipulates plant cell is better understood. On the other hand, no homologous sequence is found in T_L-DNA and T-DNA region of pTi. Therefore, T_L-DNA is of particular interest. By using genetic and molecular analysis, four genes in

the T_L-DNA were shown to play crucial roles in hairy root formation. The four root loci (*rol*) were named *rolA*, *rolB*, *rolC*, and *rolD*, respectively (Fig. 1-4) (White et al., 1985). Following briefly summarize findings about the four genes.

1.3 RolA

rolA is a 303 bp, no-intron gene (GenBank: K03313.1, X12579.1). Its protein contains 100 amino acids and is a basic protein (isoelectric point = 11.2) (UniProtKB/Swiss-Prot: P11888) (Slightom et al., 1986; Levesque et al., 1988). *RolA* was discovered through morphological observation of *Kalanchoe diargemontiana* hairy roots induced by *A. rhizogenes* Tn-5 inserting mutant (White et al., 1985). The Tn-5 inserting-*rolA* mutant (*rolA* interrupted mutant) induces hyper-hairy roots with longer root length when comparing to wild type *A. rhizogenes*-induced ones. On the other hand, morphological differences of regenerated plants that induced by *rolA*-transformed hairy roots of bittersweet (*Solanum dulcamara* L.) and tomato (*Lycopersicon esculentum* Mill.) were also reported (McInnes et al., 1991; Van Altvorst et al., 1992). These plants all exhibited shorter plant height, reduced internode length, extensive wrinkle leaves, retard flowering time and severe male infertility. In order to understand how and why one gene was capable to cause the massive changes in plant morphologies, studies had been focusd on its spatial and temperal regulations in regenerate plant (Sun et al., 1991; Van Altvorst et al., 1992; Armando Aguado-Santacruz et al., 2009).

Promoter region of *rolA*, which spans 638 bp upstream of its translation start site, has been studied extensively (Carneiro and Vilaine, 1993; Guivarch et al., 1996). When *rolA* was expressed under the control of its full-length promoter, it was expressed throughout the whole regenerated plant in vegetative stage with all the chimeric phenotypes, like wrinkle leaves and reduced internode. Moreover, when leaf discs of the

regenerate plants were cut and put on hormone-free medium, roots form spontaneously (Guivarch et al., 1996). However, when -638 to -473 region was deleted, the spontaneous root formation disappears and *rolA* was expressed only in companion cells of the phloem. Therefore, this region is thought to comprise of tissue-type regulation (Guivarch et al., 1996). When *rolA* promoter region was further deleted from -638 to -336, wrinkle leaves and reduced root phenomenon of the regenerated plant vanished. This indicates that -473 to -336 is responsible for the two phenotypes (Carneiro and Vilaine, 1993). Deletion of *rolA* promoter from -638 to -200 results in significantly reduced *rolA* expression in leaves and low expression in stem phloem. Nevertheless, the low expression in stem was still sufficient to inhibit internode elongation. Therefore, region -336 to -200 consists of phloem-specific elements and is able to alter stem morphology (Guivarch et al., 1996). The 100 bp upstream of *rolA* translation start site shows an unexpected character: the prokaryotic origin nucleotides are recognized by eukaryotic plant cell and spliced out in the mRNA level (Xue et al., 2008). As qRT-PCR results indicated, plant cells recognize the 3'AG (at position -3) and 5'GT (position -73, and -76 respectively) sites of the pre-*rolA* mRNA and spliced it out to make a mature one (Xue et al., 2008). The mature *rolA* mRNA is important to produce functional RolA protein since the *in vitro* test showed that the translation of pre-*rolA* mRNA was at least 10-20 times weaker than that of the mature one. Moreover, 3'AG mutant is a null mutant that did not show ectopic morphology in *Arabidopsis* (Magrelli et al., 1994). In conclusion, *rolA* promoter controls not only the tissue specific expression but also the chimeric morphology of the regenerated plant.

On the other hand, mRNA levels as well as protein functions of *rolA* have also been studied. The mRNA level of *rolA* had the highest level in stem and this content was more than five and fifty times in leaves and in roots, respectively (Carneiro and

Vilaine, 1993). These data consist with the fact that the -336 to -200 promoter region of *rolA* controls the gene in a stem-specific manner (Carneiro and Vilaine, 1993). The protein product of *rolA* mRNA is a 100 amino acids with molecular weight of 11.4 kDa. Also, amino acid sequence analysis indicated that RolA protein is a basic protein with isoelectric point of 11.2 (Slightom et al., 1986; Levesque et al., 1988). The basic nature of RolA leads to the hypothesis that it may harbor DNA binding capacity (Rigden and Carneiro, 1999). This hypothesis was strengthened by the fact that RolA structure adopts the papillomavirus E2 DNA-binding domain by computer simulation model (Rigden and Carneiro, 1999). If RolA is really a DNA-binding protein, it is expected to localize in the nuclei. However, the product of *RolA::GUS* fusion protein showed the GUS activity was highest in microsomes and plasmamembrane region but low in nuclei (Vilaine et al., 1998). Moreover, no studies have found nuclear localization signals in RolA sequence. Therefore, whether RolA protein is a DNA-binding protein as well as its biological function remains to be elucidated.

1.4 RolB

Gene *rolB* is 780 bp long, and its protein product contains 259 amino acids (GenBank: K03313.1, UniProtKB/Swiss-Prot: P20402). It shares homology with RolB in Tr-DNA (the two gene have the same name because of the homology) (UniProtKB/Swiss-Prot: P15397).

Among all the *rol* genes, *rolB* affects hairy root morphology most dramatically in many plants. In *K. diargremontiana*, the Tn5-interrupted *rolB* mutant resulted in avirulent trait (White et al., 1985). Tobacco harboring 35S *rolB* itself was sufficient to induce hairy root syndrome, which confirms the crucial role of *rolB* (Cardarelli et al., 1987). In transgenic plants, *rolB* stimulated the formation of flower and root

meristemoids in tobacco thin cell-layers (Capone et al., 1989; Altamura et al., 1994). The meristomoid development has been known to be regulated by auxin (De Smet et al., 2007). Therefore, *rolB* is suggested to be involved in auxin homeostasis (Capone et al., 1989). This hypothesis is strengthened by the fact that the promoter region of *rolB* was induced by auxin (Maurel et al., 1990). Besides the auxin-induced character, *rolB* promoter has many other intriguing traits. First, the promoter was active not only in the central cylinder of regenerate embryo but also all types of meristem in the regenerated tobacco and regenerated carrot (Capone et al., 1989; Schmulling et al., 1989; Altamura et al., 1991). Second, its expression was organ-specific. The expressing level of the *rolB* promoter was high to low in the order of stem, root and leaf, respectively (Capone et al., 1989; Chichiricco et al., 1992). Third, each promoter fragment of the *rolB*, defined by restriction sites, harbors different functions. For example, fragment -623 to -471 enables the downstream gene to express in root cap and protoderm. Deletion of this fragment largely reduced expressing level of the reporter gene (Capone et al., 1994). Fragment -341 to -306 is crucial for the promoter activation and defines the expression in root tip and meristem of vascular tissue. Another example is fragment -218 to -158. Deletion of this region results not only in the vanish signal in vascular meristematic cells but also in express signal in protoderm. The deletion of fragment -158 to -85 where deletion of this fragment causes vanish expressing signals in dermatocalyptogen and cortex (Capone et al., 1994).

Aside from the promoter region of *rolB*, its biological function has also gained a lot of research interest. Reflecting the fact that promoter *rolB* is induced by auxin and that *rolB* may be involved in auxin homeostasis, investigation of the biological function of *rolB* have been focused on its relationship with auxin. The protein product of *rolB* was first suggested to be a 3-glucosidase which can release IAA (indole-3-acetic acid),

one kind of active auxin, from IAA-beta-glucoside (indole-3-acetyl-beta-glucoside) (Estruch et al., 1991). This point of view was supported by the observation that higher IAA and lower GA content were found in protein RolB-expressing anther (Spena et al., 1992). Nevertheless, further study showed that neither endogenous free IAA pool, nor the rate of IAA biosynthesis and metabolism were altered in *rolB*-transformed tobacco (Nilsson et al., 1993; Schmülling et al., 1993). In addition, the morphology of *rolB*-expressing transgenic tobacco did not resemble that of IAA overproduction ones (Nilsson et al., 1993). Therefore, the hypothesis that protein RolB is a 3-glucosidase which release free auxin in plant cell is not likely to be true. Though it may not play a role in either active auxin release or auxin biosynthesis or metabolism, RolB could instead affects auxin transportation. This is supported by the fact that protein RolB not only is found in the plasma membrane but also increases the amount of auxin binding to tobacco plasma membrane (Filippini et al., 1994; Filippini et al., 1996). Furthermore, protein RolB was shown to possess tyrosine phosphatase activity when purified exogenously from *E. coli* (Filippini et al., 1996). Thus, it is suggested that RolB affects auxin transportation through the kinase / phosphatase cascade signal transduction (Filippini et al., 1996). However, the study did not show the tyrosine phosphatase activity of RolB *in vivo*. Thus, whether *rolB* functions as a tyrosine phosphatase in plant cell remains to be elucidated.

1.5 RolC

RolC is a 543 bp gene (GenBank: K03313.1). Its protein is 20 kDa and contains 180 amino acids (UniProtKB/Swiss-Prot: P20403). Hairy root induced from *K. kiagremontiana* by Tn5-interrupted *rolC* mutant *A. rhizogenes* shows attenuate growth after initiation (White et al., 1985). Regenerated tobacco harboring *rolC* under its own

promoter show short plant height, reduced apical dominance, early flowering time, small size flower, and poor pollen production (Schmulling et al., 1988). Like other *rol* genes discussed above, *rolC* alone affects plants' morphology drastically. Thus, many studies have been conducted to determine its biological functions.

Studies of the *rolC* promoter can be divided into two parts. One is the regulatory mechanism of the *rolC* promoter; another is the plant nucleus proteins capable of binding to the promoter region of *rolC*. Promoter analysis using GUS as a reporter in regenerate tobacco showed that *rolC* promoter is phloem- and root- specific (Schmulling et al., 1989; Sugaya et al., 1989). A further study demonstrated that the promoter region was responsible for phloem-specific expression lies within -153 to +1 (Sugaya and Uchimiya, 1992). Moreover, the -135 to -94 region of the *rolC* promoter, which overlaps with phloem-specific region, is also induced by sucrose (Yokoyama et al., 1994). Since high levels of sucrose is likely to be found in the phloem, it will be interesting to know the correlation between *rolC* expression and sucrose concentration. On the other hand, multiple plant proteins were found to be capable of binding to *rolC* promoter. These plant proteins include the 43 kDa, RCS2 protein (*rolC* ssDNA-binding protein 2), AII protein and BI protein (Matsuki and Uchimiya, 1994; Fujii, 1997). The latter two were shown to bind from -203 to -92. Still another protein, protein Ava S, was found to interact with *rolC* promoter. However, Ava S only bound to single strand DNA of the promoter from -94 to +23 (Suzuki et al., 1992).

Attempts to find the biological functions of RolC have not been succeed. RolC-specific antibody experiments demonstrated that it lies in the soluble, cytosolic fraction of the transgenic cells (Estruch et al., 1991; Oono et al., 1991). In 1991, Estruch et al. demonstrated that RolC harbors cytokinin-beta-glucosidase activity *in vitro* using recombinant protein system (Estruch et al., 1991). This indicates that plant morphology

affected by RolC may be due to the fact that more active cytokinin was produced. However, attempts to confirm this idea *in vivo* had shown contradictory results. Nilsson and coworker found that the cytokinin levels were low in RolC-expressing tobacco cell, whereas abscisic acid levels were high (Nilsson et al., 1993). Faiss et al. (1996) also found that the free cytokinins level did not change in any tissue and they did not observe cytokinin-beta-glucosidase activities of RolC as well (Faiss et al., 1996). Thus, the biological function of RolC remains unknown to date.

1.6 RolD

Gene *rolD* is a 1035 bp gene (GenBank: K03313.1). Its protein contains 344 amino acids and served as a NAD⁺-dependent ornithine cyclodeaminase in pRi1855 (Trovato et al., 2001). *RolD* was first characterized as the Tn5-interrupted *rolD* mutant induced retarded hairy root growth and increase callus phenotype in *K. kiagremontiana* (White et al., 1985). Afterward, the effect of *rolD* in hairy root initiation in tobacco was also studied. Surprisingly, *rolD* was found not necessary for hairy root induction in tobacco system (Vilaine and Cassedelbart, 1987). Therefore, whether *rolD* is required for virulence seems to be plant species-dependent. Interestingly, though not obligate for hairy root initiation, regenerate tobacco harboring *rolD* shows early flowering followed (at the stage of 10-11 internodes) by rapid growth of numerous lateral inflorescences (Mauro et al., 1996). Adventitious root meristem was also increased in *rolD* expressing *A. thaliana* (Falasca et al., 2010).

Due to the effects *rolD* have on root meristem, studies have investigated its promoter region. Shorten *rolD* promoter (-325 to -1) was shown to exhibit root-specific expressing pattern in regenerate tobacco (Leach and Aoyagi, 1991). This is further confirmed by the fact that the ratio of root to leaf expressing level of mature regenerate

tobacco is 28 and 24 when using -1271 to -1 (full length) and -426 to -1, respectively (Elmayan and Tepfer, 1995). Since then, the -325 to -1 region of *rolD* has been used as a root-specific promoter (Kamo, 2003; Tamot et al., 2003; Jayaraj et al., 2008).

The protein function of *rolD* is also characterized. Trovato *et al.* found that the protein product of *rolD* is a NAD⁺-dependent ornithine cyclodeaminase, an enzyme that converts ornithine to proline (Trovato et al., 2001). Proline accumulation may be a defense response connected to biotic and abiotic stresses (Mauro et al., 1996; Trovato et al., 2001). Therefore, it will be interesting to know whether this defense response is really altered in hairy root induced by *rolD* deficient mutant.

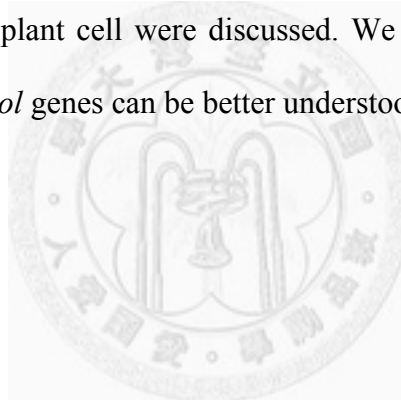
1.7 Research strategies

As mentioned above, only *rolD* gene has known functions so far; protein product of *rolA*, *rolB*, and *rolC* still remain poorly understood. Considering their crucial role in hairy root formation, and the potential of hairy root for the production of secondary metabolites, unveiling the functions the *rol* genes have in hairy root will give a fundamental progress to plants as well as bacteria biology.

From our literature review, it is surprising that although many attempts have been made to elucidate *rol* genes' function, few of them chose hairy root system as their model. On the contrary, most of them used regenerate plants as their targets. Also, most previous studies that used hairy root as their material focused on hairy root initiation rather than the architecture of hairy root. Since hairy root have been view as the most powerful plant secondary metabolites-producing system, understanding how *rol* genes affect hairy root architecture may provide new insights of how to improve the quantity of the hairy root tissue. Moreover, researchers have turned their interest into single clone, high quantity secondary metabolite production for the past decade (Bulgakov,

2008; Ono and Tian, 2011), when many comprehensive analyses, the -omics data, became mature. This leads to poor comprehensive information of how plant cell is manipulated by the *rol* genes, and hindered the elucidation of the *rol* genes' biological function.

Therefore, this study focused on hairy root system induced by *rol* gene-deficient *A. rhizogenes* rather than the regenerate plant induced from it. Starting from morphological differences analysis, attempts were made to elucidate how individual *rol* genes affect hairy root architectures. Then, microarray and qRT-PCR technology was used to identify how plant genes were manipulated by individual *rol* gene. Combining morphological and gene expression data, the underlying molecule mechanisms of how individual *rol* genes affect plant cell were discussed. We hope that by these data, the biological functions of the *rol* genes can be better understood.



Chapter 2. Materials and Methods

2.1 Plant materials and growth conditions

Nicotiana tabacum L. cv. Wisconsin 38 was used in this study. The seeds were surface sterilized by 70% (v/v) ethanol once followed by washing with sterilized water three times. Then, 1% sodium hypochlorite containing 0.01% Tween-20 was used to further surface sterilize the seed once followed by washing with sterilized water until no surfactant remained. The surface-sterile seeds were deposited onto ½ MS plate (half-strength Murashige and Skoog medium containing 3% sucrose, pH 5.8 (adjusted by KOH), and 0.3% (w/v) phytigel). The seeds were grown under 22 °C, 400 $\mu\text{moles/m}^2/\text{s}$ light intensity with 14 h light / 10 h dark photoperiod for 3 weeks. Afterward, the young plants were transferred onto ½ MS containing-107 x 94 x 96 mm culture box and grown for another 5 weeks before the bacteria infection.

2.2 Bacteria and growth conditions

In this study, wild-type *Agrobacterium rhizogenes* strain A4 and its derivatives were used. The derivatives: ΔrolA , ΔrolB , ΔrolC , and ΔrolD *A. rhizogenes* strain A4 (*rolA*, *rolB*, *rolC*, and *rolD* deleted mutant, respectively) were kindly provided by Jung-Hao Wang. These bacteria were constructed using homologous recombination techniques. *A. rhizogenes* strain A4 derivatives were grown on YEB plate (5 g / L tryptone, 1 g / L yeast extract, 5 g / L nutrient broth, 5 g / L sucrose, and 0.49 g / L $\text{MgSO}_4 \cdot 7\text{H}_2\text{O}$, pH 7.2, solidified with 15 g / L agar) at 26 °C. Single colony was selected and sub-cultured in glass tube containing 3 mL YEB at 26 °C, 130 rpm. For growth curve analysis, OD_{600} were recorded every 3 hours until the observation values did not increase. Three biological replications were performed for each genotype.

2.3 Genotype confirmation for *A. rhizogenes* strain A4 derivatives

The genotype of wild-type *A. rhizogenes* strain A4 and its derivatives were checked routinely to ensure no contamination existed during the experiment. DNA of these bacterium were extracted using UniversAll Tissue PCR kit (Yeastern, Taiwan) by dipped a single colony into 10 μ L UniversAll extraction buffer then incubated at 95 $^{\circ}$ C for 10 min. Then, the extractant became ready-to-use template. The template was then confirmed by PCR with primer pairs shown in Table 1. The pK18HRrol check primers (red arrows in Fig. 2-1) were designed to be flanked by the respective *rol* gene (blue bar in Fig. 2-1). Therefore, the non-deleted *rol* genes will give PCR amplified fragments of about 1500 bp, while the amplified fragments of deletion of the *rol* genes will be about 500 bp. The 10 μ L PCR solution containing 5 μ L of 2.0 fold and 1.5 mM $MgCl_2$ *Taq* DNA Polymerase Master Mix Red (Ampliqon, Denmark), 1 μ L extracted DNA, and 4 μ L primer mix (final 0.2 μ M each). PCR was performed as follow: 95 $^{\circ}$ C 5 min, 35 cycles of 95 $^{\circ}$ C 30 s, 55 $^{\circ}$ C 30s, 72 $^{\circ}$ C 100 s, then 72 $^{\circ}$ C for 10 min.

2.4 Hairy root induction

Single colony of *A. rhizogenes* strain A4 and its mutant $\Delta rolA$, $\Delta rolB$, $\Delta rolC$, and $\Delta rolD$ were picked, inoculated in test tube containing 3 mL YEB medium, and cultivated at 26 $^{\circ}$ C, 130 rpm for 2 days. The bacteria culture was then diluted by $\frac{1}{2}$ MS medium to 0.1 units of OD_{600} to make infection medium. The 8-week-old *N. tabacum* leaves were cut into approximately 1 cm^2 and the basal side was slightly dipped into the infection medium. Aside from dipping, 0.4 μ L of the infection medium was injected to the main vein of the leaf disc in hairy root initiation ability test to control the quantity and position of infection. Either way was used, the bacteria-containing leaf discs were

then planted onto $\frac{1}{2}$ MS plate for co-inoculation at 22 °C for 3 days in dark. After co-inoculation, the dipped infected-leaf discs were washed three times by 200 ppm cefotaxime-containing $\frac{1}{2}$ MS medium to reduce the bacterium titer then implanted to 300 ppm cefotaxime-containing $\frac{1}{2}$ MS ($\frac{1}{2}$ MS+Ce) plate. On the other hand, the bacterium injected-leaf discs were put directly onto $\frac{1}{2}$ MS+Ce plate. After 21 days post infection (dpi), hairy root emerged from the infected leaf disc was cut and placed onto a 6 cm diameter, fresh $\frac{1}{2}$ MS+Ce plate. Only one single root of each leaf disc will be transferred onto the new plate to guarantee clone independency. Hairy roots induced by *A. rhizogenes* strain A4 and its *rol* gene-deficient mutant, $\Delta rolA$, $\Delta rolB$, $\Delta rolC$, and $\Delta rolD$ were designated HR WT, HR $\Delta rolA$, HR $\Delta rolB$, HR $\Delta rolC$, and HR $\Delta rolD$, respectively. The independent hairy root clones were sub-cultured every two weeks. Moreover, at least 3 succeeded sub-culturing onto a fresh $\frac{1}{2}$ MS+Ce plate were conducted to eliminate *A. rhizogenes* contamination before any measurements were performed.

2.5 Hairy root initiation test

Hairy root initiation was measured by RL ratio (the primary hairy root number per leaf disc) and DREPI (days of the first root emergence post infection). The RL ratio is defined as the primary root number per leaf disc at 21 days post infection, while the DREPI is defined as the days of the first root emergence post infection during 21 dpi (Swain et al., 2010). The better root initiation was defined as early DREPI and high RL ratio. In this experiment, each leaf was cut into 5 pieces and infected by either WTA4 or its derivatives. Thirty independent leaves were used each time. However, some leaf discs were abandoned due to contamination. Therefore, the biological replications of

WT and $\Delta rolA$, $\Delta rolB$, $\Delta rolC$, and $\Delta rolD$ used in this test were 60, 60, 60, 45, and 52, respectively.

2.6 Hairy root genotype confirmation

After succeeding at least 3 times in sub-culturing, genotypes of the hairy root were confirmed using primers described above (Table 2-1). Tobacco *ACTIN-9* primers were used as a positive control of the materials, and *VirA* primers were used as a negative control to evaluate whether the bacteria had been eliminated completely. The genomic DNA of hairy roots were extracted by Wizard Genomic DNA Purification Kit (Promega, USA) then adjusted to 2.5 ng/ μ L. The 10 μ L PCR solution containing 5 μ L of 2.0 fold and 1.5 mM $MgCl_2$ *Taq* DNA Polymerase Master Mix Red (Ampliqon, Denmark), 4 μ L (10 ng) genomic DNA, and 1 μ L primer mix (final 0.2 μ M each). PCR was performed as follows: 95 °C 5 min, 30 cycles of 95 °C 30 s, 55 °C 30s, 72 °C 100 s, then 72 °C for 10 min.

2.7 Analysis of hairy root architectures

The parameters used for hairy root architecture analysis were main root length (MRL), branch root number (BRN), total branch root length (TBRL), and branch root density (BRD) (Hernández-Mata et al., 2010). These parameters were measured after 18 days of sub-culturing. The sub-culture was performed by cutting 1.5 cm of hairy root from the root tip onto a fresh $\frac{1}{2}$ MS+Ce plate (6 cm diameter) then cultured at 22 °C in dark. The position of the incision root was marked on the plate (dash line in Fig. 2-2). Main root indicates the same root extended directly from the marked root, while branch root is defined as the roots directly extruded from the main root (shown in asterisk in

Fig. 2-2). Total branch root length is the length of all branch roots. Branch root density means the branch root number per cm of the main root (cm^{-1}).

2.8 Statistical analysis

Statistical analysis were performed by R program version 2.14.1 (R Development Core Team, 2011).

The DREPI and RL ratio data were first analyzed by the Shapiro-Wilk normality test but both were not normally distributed under the significant level $\alpha = 0.05$ (data not shown). Therefore, nonparametric methods were used for significant test. Significant effect of group was tested by Kruskal Wallis method and Mann-Whitney U tests with Bonferroni correction as the post-hoc (Bonferroni, 1936; Kruskal and Wallis, 1952; Kruskal, 1957).

The parameters of hairy root architectures (MRL, BRN, TBRL, and BRD) were analyzed statistically using permutation tests of ANOVA with 1000 replications because the population distribution did not obey normal distribution. This may occur due to the small population used in this study. If insertion position of the T-DNA were taken into account, each gene must be inserted to make the complete hairy root population. To achieve the complete hairy root population, at least 4.5×10^9 independent clones have to be established (every space between two nucleotide have to be inserted once) (*Nicotiana tabacum* (common tobacco) genome view 2012), which surpass the maximum loading of our work. However, we tried to establish as much clones as we could in this study. More than 50 independent hairy root clones were used in each group (see 2.7 Analysis of hairy root architectures). Permutation test was chosen to test if different groups come from the same distribution under 95% confidence level because it does not assume normality and homogeneity of variance of the data; which was the case

of our data. The permutation test was conducted as follow: a F-value was obtained using ANOVA comparing one of the *rol*-gene deficient induced HR and WT HR. Then, the groupings of all the observations were permuted. The permuted data was then analyzed by ANOVA and obtained another F-value. The permutation were performed 1000 times, and hence 1000 more F-value. The percentage of F-value larger than or equal to the original one was reported as the permuted *p*-value. Therefore, the smaller the *p*-value was, the more significant between the groups. All the comparisons were conducted against HR WT.

2.9 RNA extraction

To bypass gelling agent contamination during hairy root tissue, hairy root were cultured in liquid medium before sampling. Each hairy root was cut 1.5 cm from the root tip then put into a 50 mL ½ MS broth in a 250 mL flask, and cultured in the dark at 22 °C for 14 days. After the culturing, each hairy root was put onto a clean paper towel to eliminate the medium before putting into a liquid nitrogen pre-freezed mortar. The tissue was then homogenized by pestle and mortar to fine powder. Before thawing, the tissue powder was put into Trizol reagent (Invitrogen, USA) then stored at -80 °C. Each clone of hairy root powder was stored in Trizol in an independent eppendorf. After all the samples were collected, at least 24 independent hairy root samples in Trizol reagent of HR WT were pooled to make one mixed sample. The HR $\Delta rolA$, HR $\Delta rolB$, HR $\Delta rolC$, and HR $\Delta rolD$ were done in the same way. Total RNA extraction of the mixed sample was performed by Direct-zol RNA MiniPrep (Zymo research, USA) follow the manufacture's instruction manual.

2.10 Microarray labeling, scanning, and data extracting

The qualities of the total RNAs were checked by Agilent 2100 bioanalyzer (Agilent, USA). 0.2 µg of total RNA was amplified by a Low Input Quick-Amp Labeling kit (Agilent Technologies, USA) and labeled with Cy3 or Cy5 (CyDye, Agilent Technologies, USA) during the *in vitro* transcription process. Cy-labeled cRNAs were hybrid to dual-channel Agilent Tobacco Oligo 4x44K Microarray (Agilent Technologies, USA) then scanned with an Agilent microarray scanner (Agilent Technologies, USA) at 535 nm for Cy3 and 625 nm for Cy5. The scanned images were analyzed, normalized by rank-consistency-filtering LOWESS method using Feature extraction 10.5.1.1 software (Agilent Technologies, USA). For comparison between HR WT and HR $\Delta rolA$, as well as HR WT and HR $\Delta rolD$, one replicate was done. For comparison between HR WT and HR $\Delta rolB$, as well as HR WT and HR $\Delta rolC$, two biological replicates were performed. Also, the two biological replicates were analyzed in a dye-swap manner. Genes consistent down regulated with a two-fold cut off threshold in HR $\Delta rolB$ / HR $\Delta rolC$ compared to that in HR WT were selected and listed for further ontology analysis (data not shown).

2.11 Gene ontology of microarray data

The extracted genes were analyzed by Gene Ontology (GO) Analysis Toolkit and Database for Agricultural Community (agriGO) (Du et al., 2010). Using Singular Enrichment Analysis (SEA) with default setting, the biological process differences between HR WT and HR $\Delta rolB$ were evaluated, as well as between HR WT and HR $\Delta rolC$ according to their probe name. The default settings of SEA analysis are described below. The Fisher method was used for statistical test, Yekutieli (FDR under

dependency) method was used for multi-test adjustment method, significant level were set at 0.05 and the minimum number of mapping entries was 5, and complete GO database was used. Gene ontology in terms of biological process was reported as a diagram with explanation shown in Fig. 2-3. In general, each block represents a specific gene ontology group, and the scope of the group shrinks from top to bottom. Therefore, the lower the block represented a more specific GO the group. The relationship of the blocks between two adjacent rows is expressed by different kinds of arrows (Fig. 2-3). The significant level was expressed within parentheses.

2.12 qRT-PCR

Probe names extracted from GO analysis were blasted to search the best fits mRNA and / or DNA in the NCBI database. Specific primers were designed according to the above information. The primers were named after their NCBI accession numbers as shown in Table 2-2. These primers were first tested using HR WT cDNA template to see if only one peak exists in the melting curve, and whether the C_T value lies within 35 cycles. After the preliminary test, the primers were used for expression level examination.

In experiment comparing HR *ΔrolC* and HR WT, 3 independent clones were chosen. On the other hand, due to low biomass and poor viability, only 2 HR *ΔrolB* clones were analyzed with another two independent HR WT clones. The two-week old hairy roots after sub-culturing into liquid ½ MS medium and were used for total RNA extraction by Direct-zol RNA MiniPrep (Zymo research, USA). The first-strand cDNA was synthesized using 1.5 ng of total RNA with GoScript Reverse Transcription System (Promega, USA). The extending temperature was 42 °C and RNasin was used during the reverse transcription. The qRT-PCR analyses were performed by CFX384 real-time

PCR detection system with iQ SYBR green supermix (Bio-Rad, USA). For each test, 3 technical replications were performed. The qRT-PCR program was: 95 °C 3 min; 40 cycles of 95 °C 10 sec, 55 °C 30 sec, plate reading; 95 °C 10 sec; melt 65 to 95 °C, increment 0.5 °C every 5 sec, plate reading. *TAC-9* (tobacco *ACTIN-9*) and *beta-TUBULIN* were used as control genes. Permutation test was used for statistic analysis as previously described.



Chapter 3. Results

3.1 Genotype confirmation of *rol* gene-deficient *A. rhizogenes* strain A4

A. rhizogenes strain A4 and its derivatives were used in this study. The derivatives were: $\Delta rolA$, $\Delta rolB$, $\Delta rolC$, and $\Delta rolD$ *A. rhizogenes* strain A4 (*rolA*, *rolB*, *rolC*, and *rolD* deleted mutant, respectively) kindly provided by Jung-Hao Wang. These strains were constructed using homologous recombinant techniques (unpublished data). The genotype of *A. rhizogenes* strain A4 and its derivatives were checked periodically during this study by amplified their DNA using pK18HR*rol* check primers. The designation of pK18HR*rol* check primers was interpreted in Fig. 3-1B (red arrow); the primers were flanked by the *rol* genes (blue line in Fig. 3-1B). Therefore, lacking *rol* genes resulted in smaller PCR amplified fragments (about 500 base pairs) than the wild-type ones (larger than 1500 bp). Moreover, *G3PDH* served as a bacterium control while *VirA* indicated the presence of pRi, both of which had products about 200 bp. Water was added in the no template group as a negative control

Results in Fig. 3-1 showed that the genotype of *A. rhizogenes* strain A4 and its derivatives were consistent with expectation as the lengths of amplified PCR fragment of the expected-deleted *rol* genes were about 500 bp and the undeleted larger than 1500 bp (Fig. 3-1). Existence of the *G3PDH* and *VirA* PCR amplified fragments confirmed the existence of *A. rhizogenes* and pRi in the materials. No amplified fragments in the no template group confirmed contamination was not present in the reagent. Overall, the results re-confirmed the genotypes of *A. rhizogenes* strain A4 and its derivatives.

3.2 Tobacco infection by *A. rhizogenes* strain A4 and its derivatives

To understand if *rol* gene deletion has any effects on bacterium growth in

YEB broth, growth curve by recording OD₆₀₀ with three biological replicates were performed (Fig. 3-2). Although wild type *A. rhizogenes* strain A4 grew slower than its *rol* gene-deficient derivatives during 12-24 h after inoculation, there was no significant differences between all groups when incubate longer than 24 h in YEB broth. According to the results and previous studies (Cardarelli et al., 1987; Batra et al., 2004; Lee et al., 2007), 48 h post inoculation was chosen for tobacco infection.

3.3 Confirmation of hairy root genotype

Hairy root genotype confirmation was performed using the pK18HRrol check primer sets after the hairy roots were transferred to fresh ½ MS+Ce for at least three times. Tobacco *ACTIN-9* served as a positive control, while *A. rhizogenes VirA* served as a negative control. *N. tabacum* L. cv. Wisconsin 38 root (W38 root) were used to validated no fragment were amplified by pK18HRrol check primer. Instead of DNA template, water was added in the no template group as a reagent control. The results confirmed that the genotype of each hairy root was as expected (Fig. 3-3). In HR WT, all the PCR products amplified by pK18HRrol check primers showed the same size as that of WT A4, indicating the presence of the *rol* genes (row 2 of Fig. 3-3). Moreover, the absence of the *VirA* product and the presence of tobacco *ACTIN-9* confirmed the hairy root origin; instead of *A. rhizogenes* strain A4. In HR $\Delta rolA$, the PCR product of pK18HRrolA had smaller fragment than that of WTA4, while others had the same size (row 3 of Fig. 3-3), confirming the phenotype was correct. The same results can be seen in other types of hairy roots as well. The results confirmed the accuracy of the hairy root genotype.

3.4 Hairy root initiation test

In wild-type *A. rhizogenes* strain A4 (WTA4) infected tobacco leaf discs, hairy roots started to initiate 10 days post infection (dpi). By 21 dpi, more than 90% of the WTA4-infected leaf discs had at least one hairy root. Earlier hairy root initiation time and higher percentile of leaf discs with hairy root indicate greater induction ability. Therefore, days of the first root emergence post infection (DREPI) recorded during 21 dpi and primary root number per leaf disc (RL ratio) recorded at 21 dpi were chosen for initiation test parameters (Swain et al., 2010).

The DREPI and the RL ratio seemed to be quite different between groups tested. Figure 3-4 shows 5 representative leaf discs selected systematically according to their hairy root numbers and length at 21 dpi. It can be clearly seen that hairy root numbers, as well as its length decreased in $\Delta rolB$ and $\Delta rolC$ -infected leaf discs. To further confirm this phenomenon, statistical analysis was performed. The DREPI and RL ratio data were first analyzed by the Shapiro-Wilk normality test but both were not normally distributed under the significant level $\alpha = 0.05$ (data not shown). Therefore, nonparametric methods were used for significant test.

Significant effect of *A. rhizogenes* genotype on DREPI ($p = 1.815 \times 10^{-8}$) was analyzed by a Kruskal Wallis test. A post-hoc test using Mann-Whitney U tests with Bonferroni correction showed significant differences between WTA4 and $\Delta rolB$ ($p = 1.1 \times 10^{-3}$) and between WTA4 and $\Delta rolC$ ($p = 8.4 \times 10^{-6}$). This may be due to the fact that there were lower root emergence rate of both groups during 10-21 dpi, and that about 20% lower at 21 dpi (Fig. 3-5). Although $\Delta rolD$ showed lower root emergence rate before 16 dpi, the root emergence rate thrived after that. At 21 dpi, no significant differences existed between $\Delta rolD$ and WTA4. On the other hand, $\Delta rolA$ showed little or no differences in root emergence rate comparing with WTA4.

The Kruskal Wallis test revealed a significant effect of *A. rhizogenes* phenotype on RL ratio ($p = 1.815 \times 10^{-8}$) (Fig. 3-6). Mann-Whitney U test adjusted with Bonferroni correction revealed the significant differences between WTA4 and $\Delta rolB$ ($p = 1.1 \times 10^{-3}$) and between WTA4 and $\Delta rolC$ ($p = 8.4 \times 10^{-6}$).

The statistical analysis confirmed that the hairy root initiation ability in $\Delta rolB$ and $\Delta rolC$ were impaired when comparing to WTA4.

3.5 Measurements of hairy root architecture

Morphology of HR WT, HR $\Delta rolA$, HR $\Delta rolB$, HR $\Delta rolC$, and HR $\Delta rolD$ were shown in Fig. 3-7. Five independent hairy root clones of each genotype were selected by systematic sampling according to their main root length (MRL) 18 d after sub-culturing. The population of HR $\Delta rolB$ and $\Delta rolC$ seemed to show growth retardation. When comparing the fourth picture of each group, HR $\Delta rolB$ and HR $\Delta rolC$ showed much shorter MRL. Moreover, the branch root development of the two populations seems to be retarded, as shown in the first picture in each group, although the population distributed a large variation. To understand if there are any statistic significant differences among the genotype of the hairy root, several parameters including main root length (MRL), branch root number (BRN), total branch root length (TBRL), and branch root density (BRD) were analyzed.

The results of main root length (MRL) analysis showed significant differences between HR WT and HR $\Delta rolC$ ($p = 9.99 \times 10^{-4}$), as well as HR WT and HR $\Delta rolD$ ($p = 9.99 \times 10^{-3}$) (Fig. 3-8B) by permutation test using ANOVA with 1000 replications. The population distribution of HR WT showed skew-to-right normal distribution with peak around MRL 5 cm (Fig. 3-8A WT). About 30% of the clones belonged to this group,

while less than 10% had MRL less than 5 cm or longer than 10 cm. Similar skew-to-right normal distribution can be seen in HR $\Delta rolC$ (Fig. 3-8A $\Delta rolC$). However, about 35% of the HR $\Delta rolC$ clones had MRL less than 5 cm, which was very different from that of HR WT. This phenomenon was more pronounced in MRL 0-2 cm. Moreover, the percentage of the observations showing MRL longer than 10 cm was also fewer than that of HR WT. The population distribution of HR $\Delta rolD$ was similar to that of HR $\Delta rolC$ (Fig. 3-8A $\Delta rolD$) with increased population with shorter MRL value when comparing with HR WT. On the other hand, although HR $\Delta rolB$ also showed similar population with MRL less than 10 cm, no significant differences existed between HR $\Delta rolB$ and HR WT ($p = 0.12$, Fig. 3-8B). This may due to the fact that about 20% of HR $\Delta rolB$ and HR WT had MRL value larger than 10 cm, while only about 10% was observed in HR $\Delta rolD$. The population of HR $\Delta rolA$ was similar to that of HR WT (Fig. 3-8A, HR $\Delta rolA$ vs. HR WT), and no significant difference was observed ($p = 0.08$). In conclusion, increased population with shorter MRL value resulted in main root length impairing of HR $\Delta rolC$ and HR $\Delta rolD$ when comparing with HR WT.

The branch root number (BRN) of HR $\Delta rolB$ and HR $\Delta rolC$ were significantly different from that of HR WT (p -value = 7.99×10^{-3} and 9.99×10^{-4} , respectively) (Fig. 3-9B). A dramatic difference can be seen in HR $\Delta rolC$, where all the hairy roots observed had less than 30 branch roots. Moreover, the BRN of more than half of the population was less than 2, indicating that branch root development may be drastically impaired in HR $\Delta rolC$. Meanwhile, the BRN of almost 60% of the HR $\Delta rolB$ was less than 5. This population was about twice more than that of HR WT. HR WT showed steady decrease in BRN from 0-20 with little percentage having branch root larger than

30, which was also the case in HR $\Delta rolA$ and HR $\Delta rolD$. Therefore, no significant differences were shown between HR $\Delta rolA$ and HR WT (p -value = 0.86), as well as between HR $\Delta rolD$ and HR WT (p -value = 0.55). In conclusion, when comparing to HR WT, HR $\Delta rolB$ and HR $\Delta rolC$ showed significant differences.

Other than branch root number, another parameter used to estimate branch root architecture was total branch root length (TBRL). In this analysis, significant differences were observed between HR WT and HR $\Delta rolB$ ($p = 4.39 \times 10^{-2}$), as well as between HR WT and HR $\Delta rolC$ ($p = 9.99 \times 10^{-4}$) (Fig. 3-10B). As can be indicated in population distribution, TBRLs were drastically decreased in both groups (Fig. 3-10A). The result further strengthens the idea that branch root development may be impaired in HR $\Delta rolB$ and HR $\Delta rolC$.

Another parameter used to measure branch root architecture was branch root density (BRD), which was defined as the number of branch root per centimeter of main root. HR $\Delta rolC$ and HR WT ($p = 9.99 \times 10^{-4}$) but not HR $\Delta rolB$ and HR WT ($p = 7.89 \times 10^{-2}$) showed significant differences (Fig. 3-11B). This may be explained by the fact that the range of the outliers in HR $\Delta rolB$ was larger than that of HR $\Delta rolC$ (Fig. 3-11A). Moreover, the BRD 0-0.5 of HR $\Delta rolC$ was twice than that of HR WT. On the other hand, there was only 33% more of BRD 0-0.5 HR $\Delta rolB$ (Fig. 3-11A). Although HR $\Delta rolD$ also showed 33% more in the BRD 0-0.5 than that of HR WT, more BRD value larger than 3.0 was also observed. This made the HR $\Delta rolD$ population range larger than that of HR WT and increased the p -value to 0.38.

Overall, hairy root architecture analyses revealed that hairy root growth was dramatically affected in HR $\Delta rolB$ and HR $\Delta rolC$ when comparing with HR WT.

3.6 Microarray Data Analysis

To elucidate the biological functions that *rol* genes manipulated in hairy root, Agilent Tobacco Oligo 4x44K microarray were used to analysis transcriptional profiles differences between hairy roots induced by *A. rhizogenes* strain A4 and its respective *rol* gene-deficient derivatives. We first compared transcriptome of hairy roots induced by WTA4 and all respective *rol* gene-deficient derivatives. Considered the pivotal roles $\Delta rolB$ and $\Delta rolC$ had on hairy root architecture, we then performed another biological replicate by comparing the transcriptome of hairy roots induced by $\Delta rolB$ / $\Delta rolC$ and WTA4 using the same kind microarray chip in a dye-swap manner. Each microarray RNA sample was combined of at least 20 independent hairy root clones.

In comparison between $\Delta rolA$ and WTA4, 217 genes were differentially up regulated in HR $\Delta rolA$ under 2-fold cut off threshold and 352 genes were differentially down regulated (Table 3-1). On the other hand, comparison between $\Delta rolD$ and WTA4 showed that 271 genes were differentially up regulated in HR $\Delta rolD$ under 2-fold cut off threshold and 297 genes were differentially down regulated (Table 3-1).

The consistent up- and down- regulated genes from the comparison between HR $\Delta rolB$ vs. HR WT as well HR $\Delta rolC$ vs. HR WT in the two biological replicates were meshed under 2-fold cut off threshold. The number of up regulated genes in HR $\Delta rolB$ and HR $\Delta rolC$ compared with HR WT were 6 and 42; the number of down regulated genes in HR $\Delta rolB$ and HR $\Delta rolC$ compared with HR WT were 242 and 208, respectively (Fig. 3-12, and Table 3-1). The number of the constitutive expressed genes was lower in comparison with other microarray analyses. This may due to different hairy root clones have different T-DNA insertion sites and / or insertion copy number, and we used two different sets of hairy root to perform the biological replicates.

Therefore, we are more confident with the constitutive expressed genes as they may be more likely to be regulated by lacking of the *rol* genes, albeit their T-DNA insertion site and / or insertion copy numbers. The same results can be seen in the constitutive down regulated genes with minor effects. The down-regulated genes were used for gene ontology analysis as they may be positively regulated by *rolB* and *rolC*, respectively.

3.7 Gene ontology of HR $\Delta rolB$ down-regulated genes

Gene ontology of the 242 down regulated-genes in HR $\Delta rolB$ was performed using agriGO with default settings (Du et al., 2010). Half of the 242 genes have been annotated, therefore only these genes were compared. The GO terms with *p*-value smaller than 0.05 were shown in Table 3-2. To get better impression about the relationships among the GO extracted, diagram according to biological process was produced (Fig. 3-13).

Four main categories of GO were present: localization, cellular process, metabolic process, and response to stimulus. The subgroups in “localization” pin point that the lipid transport was drastically decreased in HR $\Delta rolB$ ($p = 2.95 \times 10^{-13}$). Genes included in this blocks are listed in Table 3-3. The major group “response to stimulus” contained two specific subgroups showing significant differences. These groups were “response to wounding” and “response to ethylene” ($p = 1.36 \times 10^{-4}$ and 4.43×10^{-2} , respectively; Fig. 3-13). Although there was no significant difference in the group “cellular process and metabolic process”, one of their subgroup “cellular amino acid derivative biosynthesis process” was extracted ($p = 3.35 \times 10^{-2}$, Fig. 3-13).

3.8 Gene Ontology of HR $\Delta rolC$ down-regulated genes

Gene ontology of the down regulated genes in HR $\Delta rolC$ was performed as that

described in HR $\Delta rolB$. In this case, 88 of 208 genes have been annotated. Therefore, we chose these 88 genes for further analysis. Table 3-4 provides the complete GO terms with p -value smaller than 0.05.

Three main categories of GO were present: response to stimulus, metabolic process, and localization (Fig. 3-14). The subgroups in “localization” showed that the lipid transport was drastically decreased in HR $\Delta rolC$ ($p = 6.37 \times 10^{-10}$) (Fig. 3-14 and Table 3-5). It is worth noting that the group “lipid transport” showed the smallest p -value among all GO terms in HR $\Delta rolC$ and well as in HR $\Delta rolB$. The specific sub-group extracted in metabolic process was the carbohydrate metabolic process ($p = 1.52 \times 10^{-2}$) (Fig. 3-14 and Table 3-5). Two sub-groups that were significant extracted from the group “response to stimulus” were “response to chemical stimulus ($p = 4.11 \times 10^{-3}$) and response to wounding ($p = 8.10 \times 10^{-3}$) (Fig. 3-14). Genes of these groups were listed in Table 3-5.

3.9 qRT-PCR Analysis of the Gene Ontology-extracted genes

qRT-PCR was used to confirm the results obtained from the microarray. We aimed to test the relatively down-regulated genes in HR $\Delta rolB$ / HR $\Delta rolC$ comparing to HR WT. The comparison results between HR $\Delta rolB$ and HR WT confirmed the microarray data where all the successfully tested genes showed lower expression level in HR $\Delta rolB$ than HR WT (Table 3-3, Fold change in qRT-PCR analysis). The confident level of the qRT-PCR test was high as permutation analysis showed p -value equals to 1×10^{-3} in all except primer DW003388 (p -value = 2×10^{-3}). The unsuccessful tested genes mean the genes that showed C_T value larger than 0.5 among the 3 technical replicates. These data were excluded and represented as NA in Table 3-3. Also, primers exclusively existed in GO term “cellular amino acid derivative biosynthesis process” had not been designated,

and was shown by gray background.

Comparing the expression level between HR $\Delta rolC$ and HR WT, 26 of the genes tested showed the same trend as the conclusion made in microarray analysis with small p -value (Table 3-5). The gray backgrounds in Table 3-5 represent the probes without known NCBI accessions, and no qRT-PCR data shown. Primers showed C_T value larger than 0.5 among the 3 technical replicates were excluded and thus no fold change were shown (represented by NA). Although the expression of EB684101 (belongs to carbohydrate metabolic process) and FG636940 (belongs to chemical stimulus) were 0.9363 and 0.8980 fold, respectively, in HR $\Delta rolC$ divided by HR WT, both permutation p -values were larger than 0.05 (p -value was 0.0679 for the former and 0.1568 for the latter). Therefore, these data should be abolished then test again. On the other hand, gene FG137954 (belongs to lipid transport) and AB263747 (belongs to carbohydrate metabolic process) were not differentially expressed in HR WT and showed small p -value. The expression of FG137954 and AB263747 did not obey the trend shown in microarray, and these genes should be excluded for further hypothesis generation. For $rolC$ -regulated-genes exploration, the 26 tested genes that showed the expected trends should be analyzed with higher priority.

Overall, the qRT-PCR analysis reconfirmed the accuracy of the microarray data and helped to exclude some unlikely-to-be-true cases. The information can be used in further biological function exploration of the $rolB$ and $rolC$.

Chapter 4. Discussions

4.1 *rolB* and *rolC* play crucial roles in hairy root initiation

As revealed in DREPI and RL ratio analysis (Fig. 3-5 and 3-6), our results showed that the $\Delta rolB$ and $\Delta rolC$ were less virulent to *N. tabacum* than WT A4 was. These observations are similar to the results obtained in *K. diagemontiana* where *rolB* Tn5-interrupted mutant results in avirulent traits and *rolC* interrupted mutant results in attenuate hairy root growth after initiation (White et al., 1985). However, there are some differences. For example, the *rolB* interrupted mutant resulted in avirulent traits in *K. diagemontiana*, but *rolB* deleted mutant only resulted in significantly decreased virulence in *N. tabacum*. Moreover, we did not observe the hyper-hairy root syndrome in $\Delta rolA$ in *N. tabacum*, which was the case in *K. diagemontiana* (White et al., 1985). In fact, no significant difference was shown in the RL ratio analysis between HR $\Delta rolA$ and HR WT ($p = 1.9 \times 10^{-1}$). The different hairy root initiation ability between *K. diagemontiana* and *N. tabacum* may due to their different plant origin. This point of view can be further supported by the fact that although *rolD* deletion resulted in retard hairy root growth and increase callus in *K. diagemontiana*, our results showed that *rolD* was not necessary for hairy root inducing in tobacco system, which consists with what Vilaine and colleagues had showed (Vilaine and Cassedelbart, 1987). However, the trend that *rolB* and *rolC* seem to play a major role in hairy root initiation did not change.

4.2 *rolB* and *rolC* affect hairy root architecture more drastically

To our knowledge, there is no comprehensive analysis about how *rol* genes affect hairy root architecture. In this study, we analyzed the main root length, branch root

number, total branch root length, and branch root density of the *rol* gene-deficient *A. rhizogenes* A4 induced-hairy root. From the analyses, HR $\Delta rolC$ showed impairing in all the parameters measured with the smallest *p*-value ($p = 9.99 \times 10^{-4}$) when comparing to HR WT (Fig. 3-9 to 3-12). This indicated that the development of HR $\Delta rolC$ were greatly impaired. HR $\Delta rolB$ showed reduced branch root number and total branch root length, but not in main root length and branch root density (Fig. 3-9 to 3-12). The *p*-value of the branch root density between HR $\Delta rolB$ and HR WT were 0.0789, which was slightly higher than the significant level $\alpha=0.05$. The results indicated that branch root development of HR $\Delta rolB$ were impaired. No significant difference was observed between HR $\Delta rolA$ and HR WT in hairy root architecture, nor in hairy root initiation. However, the absence of *rolA* did show hyper-hairy root morphology in *K. diargremontiana* system (White et al., 1985). Therefore, *rolA* probably plays a milder role in hairy root syndrome. Similar to HR $\Delta rolA$, only main root length was affected in HR $\Delta rolD$. The decreased MRL in HR $\Delta rolD$ reflects the observation that *rolD* interrupted mutant resulted in retard hairy root growth in *K. diargremontiana* (White et al., 1985). Taken together, it suggest that *rolB* and *rolC* that play more vital roles in hairy root syndrome.

4.3 Difficult maintenance of the HR $\Delta rolB$ and HR $\Delta rolC$ clones

We noticed that the available clones of HR $\Delta rolB$ and HR $\Delta rolC$ were decreasing during persistent sub-culturing. Many hairy root clones of both genotypes slowed or stopped elongation (but the root remained white and healthy) after multiple sub-culturing. The population decreased from 65 to less than 10 independent clones in HR $\Delta rolB$, and from 82 to less than 15 in HR $\Delta rolC$, respectively, over time. Moreover, it should be noticed that the initial population (65 and 82) had already excluded the

clones that showed slow growing rates at the beginning of hairy root emergence. This phenomenon was less pronounced in HR $\Delta rolA$, HR $\Delta rolD$, and HR WT. The ongoing population declining made us failed to have enough biomass from one independent clone for qRT-PCR analysis. Therefore, more hairy root induction should be performed if more HR $\Delta rolB$ and HR $\Delta rolC$ clones are needed for qRT-PCR analysis.

4.4 Comparison between the microarray and qRT-PCR analyses

We noticed that the expression fold change of HR $\Delta rolB$ vs. HR WT measured in qRT-PCR were consistently larger than that detected in microarray (Table 3-3 & 3-5), regardless of what the genes was tested. Similarly, the expression fold change of HR $\Delta rolC$ vs. HR WT of the qRT-PCR analysis seemed to lie within that detected in first and second microarray observed. This may resulted from two aspects: different sampling strategies and sampling size. The sampling strategy in microarray analysis was mixed sampling while individual clones were independently analyzed in qRT-PCR. Also, the mixed sample contained at least 20 clones while 2 clones were used for qRT-PCR. Therefore, more independent clones were needed for qRT-PCR test to know the population down-regulation range. However, the observations that these genes were down regulated in HR $\Delta rolB$ vs. of HR WT and / or in HR $\Delta rolC$ vs. of HR WT were true, regardless of what the experiments was used.

4.5 Biological processes manipulated in the absence of *rolB*

Our GO results did not extract any auxin-related groups (Fig. 3-12), although 4 probes did show GO term “response to auxin stimulus”. The observations that neither endogenous free IAA, nor the rate of IAA biosynthesis and metabolism were altered in *rolB*-transformed tobacco (Nilsson et al., 1993; Schmülling et al., 1993) support our finding. On the other hand, the group “response to ethylene stimulus” appears out of

expectation since no previous studies have linked *rolB* to ethylene (Fig. 3-12). Literature searching shows some interesting clues of the relationship between RolB and ethylene. First, both of them enhance auxin bind to plasma membrane (Maurel et al., 1990; Friml et al., 2002; Negi et al., 2008; Lewis et al., 2011). Second, both of them seem to have a positive regulation of wounding. The effect of ethylene on wounding (and *vice versa*) have been well demonstrated (Hamilton et al., 1990; O'Donnell et al., 1996). The GO group “response to wounding” was extracted in HR $\Delta rolB$ -down regulated genes suggest a positive regulate character of *rolB* on wounding response. Therefore, further work may focus on the ethylene content in hairy root and see if the ethylene content were lower in HR $\Delta rolB$ than that in HR WT.

Also extracted from GO analysis of the HR $\Delta rolB$ down-regulated genes was a Myb58 gene, which is a transcription activator of the lignin biosynthesis pathway (Zhou et al., 2009). Since lignin is one of the main components of cell wall, lacking Myb58 will results in cell wall biosynthesis defects. This may explain our observation that the branch root development were retarded in HR $\Delta rolB$ and that it was difficult to maintain HR $\Delta rolB$ clones because they stop to elongation (see Discussion 4.2). Future work may focus on whether the stop-to-elongation phenomenon observed in HR $\Delta rolB$ does result from cell wall biosynthesis defects.

Another gene extracted from GO analysis were ribonuclease 1 (RNS1) that has been known to regulate anthocyanin, a secondary metabolite, content in plant cell (Bariola et al., 1994). Although no reports directly suggest that anthocyanin content is higher in *rolB* expression hairy root, study does showed that the gene expression of phenylalanine ammonia-lyase (PAL) and stilbene synthase (STS), key enzymes of anthocyanin biosynthesis, was higher in *rolB* expressing grape (*Vitis amurensis*) (Kiselev et al., 2009). Therefore, two questions remain to be elucidated. The one is

whether anthocyanin content is higher in *rolB*-expression hairy root comparing to the unexpressed ones. The second is that whether *rolB* regulates secondary metabolite synthesis by RNS1.

Overall, the gene ontology analysis revealed several plausible ways of finding the biological functions of the *rolB*.

4.6 Biological processes manipulated in the absence of *rolC*

Gene ontology analysis revealed that lipid transport was affected in HR $\Delta rolC$ when compared to HR WT ($p = 6.37 \times 10^{-12}$, Fig. 3-14). In this group, 11 probes, which matched 6 GO sources, were extracted (Table 3-5). According to the gene name listed in the GO sources, we searched the TAIR database and found out that 4 of them, AT1G12090, AT1G62500, AT1G62510, and AT5G48485, locate in the endomembrane system. Another GO source, AT2G10940, locates in chloroplast thylakoid membrane, plasmodesmata, and apoplast, while GO source AT3G22142 does not have localization information. The results indicated that lipid transport in the endomembrane system was likely to be manipulated in HR $\Delta rolC$. However, previous studies pointed out that RolC lies in the soluble, cytosolic fraction of the transgenic cells (Estruch et al., 1991; Oono et al., 1991). Therefore, RolC might either regulate lipid protein indirectly or some domain of these proteins may lie within the cytosol (like membrane integrated proteins). Future works may focus on is there possible that lipid transport proteins and RolC have direct interaction.

Ten tobacco probes known to belong to GO group carbohydrate metabolic process were extracted. The probes can be referred to 8 GO sources. Six of them had been evaluated by qRT-PCR and 4 of them had been confirmed this way. The reconfirmed ones were AT1G10640, AT1G60590, AT3G61490, and AT5G55180. According to

TAIR, gene AT5G55180 belongs to O-glycosyl hydrolase family 17, locates in endomembrane system, and function in cation binding. This gene was up regulated in dark-grown seedlings when treated 6 h with 90 mM sucrose (NCBI GEO profile GDS1734 / 248100_at / AT5G55180). Since *rolC* was specifically expressed in phloem and its expression can be induced by sucrose (Schmulling et al., 1989; Sugaya et al., 1989; Yokoyama et al., 1994), it would be interesting to know if the two genes are related.

GO group response to chemical stimulus contained 21 probes with 16 GO sources. Genes belonged to this group had different functions and are stimulated by different sources (for example: pathogen, auxin, gibberellin). However, many of them seemed to response directly and / or indirectly to biotic stress like pathogen. Combining this finding and the other extracted GO group “response to wounding”, the ability of hairy root to response to pathogen might be diminished in HR $\Delta rolC$.

4.7 Deduced biological functions of *rolB*

Our results showed that *rolB* deletion resulted in retard hairy root initiation (including DREPI and RL ratio) and reduced branch root number, suggesting that *rolB* may stimulate meristem formation. This viewpoint can be strengthen by the fact that *rolB* stimulates the formation of flower and root meristemoids and that its promoter express in all types of meristem in transgenic tobacco plant (Altamura et al., 1991; Altamura et al., 1994). The observation that total branch root length was also reduced in HR $\Delta rolB$, indicated that *rolB* might also play a role in meristem maintenance. Moreover, the slow or no growing phenomenon of HR $\Delta rolB$ after multiple sub-culturing strengthened this viewpoint. Therefore, further work may focus on whether root development- and / or meristem- related genes expression are inhibited in

HR $\Delta rolB$.

Bearing the idea that *rolB* may play a role in meristem formation and / or maintenance and combining the GO analysis data, we come up with a hypothesis of how RolB acts in the plant cell (Appendix 1). In meristematic cells where high auxin level is high, auxin induces the expression of *rolB* promoter that results in increases RolB content. High content of RolB increases cell auxin sensitivity and resulted in meristem formation (gray background in Appendix 1). In order to prevent hyper-auxin level, RolB activates ethylene biosynthesis pathway by unknown mechanisms. This may be achieved by activating 1-aminocyclopropane-1-carboxylate synthase (ACC synthase) since this gene was extracted in GO analysis. Increase in ethylene resulted in expression of the down stream pathogen related genes (PR genes) and the wound response genes (lower right in Appendix 1). Some lipid transport proteins are known to be induced by wounding (García-Olmedo et al., 1995; Jung et al., 2003). Therefore, these genes may be regulated by RolB as the wounding response genes do. However, more experiments have to be done to check this hypothesis.

4.8 Deduced biological functions of *rolC*

RolC may play an important role in meristem formation and / or maintenance because HR $\Delta rolC$ was defective in main root length, branch root number, total branch root length, and branch root density consists well. Moreover, the result observed in *K. kiagremontiana* where *rolC* interrupted mutant showed attenuated hairy root growth after initiation (White et al., 1985) strengthen this viewpoint. GO analysis revealed that carbohydrate metabolic process genes includes a group of cell wall biosynthesis-related genes: polygalacturonase, glycoside hydrolase, xyloglucan:xyloglucosyl transferase, and acidic endochitinase (Fig. 3-13). Therefore, aside from meristem activity, the retard

morphology observed in HR $\Delta rolC$ may results from defect cell wall biosynthesis defects (Appendix 2). Another reason that may cause the defect morphology of HR $\Delta rolC$ may be referred to the pyruvate decarboxylase, lactate dehydrogenase, and alcohol dehydrogenase 1, which were extracted in the GO group “response to chemical stimulus”. Lack of these genes will cause malfunction in carbohydrate metabolism. It is still unknown how RolC interacts with these genes (Appendix 2). Therefore, future study may focus on these genes to elucidate how they affect root elongation.

The GO results showed that HR $\Delta rolC$ may be less response to wounding and many kinds of chemical stimulus, suggests that RolC might be sensor increase cell sensitivity to the stress. Since some lipid transport protein are known to be wound inducible (García-Olmedo et al., 1995; Jung et al., 2003), and that the cell compartmentalization of lipid transport protein and RolC do not matches (see Discussion 4.6), RolC may act indirectly with the lipid transport proteins through the response to wounding proteins (Appendix 2).

Chapter 5. Conclusion

This study was the first report that analyze the difference of the hairy root architectures among wild type- and individual *rol* gene deletion-induced ones. The results showed that comparing to HR WT, HR $\Delta rolC$ were the most affected one, which showed significant defects in all parameters analyzed. HR $\Delta rolB$ showed significant decrease in branch root number and total branch root length. HR $\Delta rolD$ showed significant retard main root length. On the other hand, only HR $\Delta rolB$ and HR $\Delta rolC$ showed significant decrease in hairy root initiation ability test. These results suggest that *rolB* and *rolC* may play a more crucial role in hairy root formation and growing. We also noted that HR WT performance was among the best in all parameter tested indicate that *rol* genes play a positive role in hairy root growth, despite their biological function remain to be elucidated.

Microarray and qRT-PCR analyses results indicated that *rolB* might positively regulate lipid transport, cellular amino acid derivative biosynthesis process, processes regarding to wound response, and response to ethylene stimulus. Meanwhile, the biological processes that may be positively regulated by *rolC* are response to wounding, response to chemical stimulus, carbohydrate metabolic process, and lipid transport. This information gives us a glance of how the biological functions were manipulated by *rolB* and *rolC* in hairy root.

Tables

Table 2-1. Primers used for genotype confirmation.

Construction	Forward primer	Reverse primer
Tobacco <i>ACTIN-9</i>	CCTGAGGTCCTTTTCCAACCA	GGATTCCGGCAGCTTCCATT
<i>VirA</i>	TACAAAGCGTGAGAGAGCA	CCAAATCTCTTTTGATTAGCTCTTCATA
<i>G3PDH</i>	ATCAAGGCTGCATCGAAC	AAGTGAGGATACGCACG
pK18HRrolA check	GGCCATTAAATTGGCACCTAC	GTGTTGATCCTGCTGCTGAA
pK18HRrolB check	TGAATGCAGCAATCTTTCACG	GCGCGATTGTCCCTGTTTAT
pK18HRrolC check	GCAGGGCGAATAGCAGTTAG	GTGGGCCAGTGCATATAGGT
pK18HRrolD check	CCGCCCACTACAATGAATTT	TCAGCCACAGGATCAGAGTG

These primers were designed by Jung-Hao Wang (Unpublished data)

Table 2-2. Primers used for qRT-PCR test

Probe name	NCBI accession	Forward primer	Reverse Primer
A_95_P000541	BQ842876	GGTTCCATCTGGCTTCCAGTGTGC	CCCTAGACCACCTTGTGCGCT
A_95_P003336	DR752062	CGAGCCATACATCAGCACGCCA	TGGGACCCCAACAGGTCAAGT
A_95_P003626	FG637828	CCTCAAGGTGGAAATAATGGCAAT	TGACTACCAGCATAAACGATTCACT
A_95_P004391	EH618856	CCCATCCAAAAGGCAAGTGCCCA	AGCAGCCTCAAGGTCAGCAACA
A_95_P005446	AB035125	AGCCGAAGTACCCGATTA	ATTGGGCTTTACGATCCTG
A_95_P007251	EF051128	GTCCGCAATCTTCAAAACCCATA	GCTCGCTGGAAGTGAATTGT
A_95_P010771	X51426	GGACTCCGTCCGCCGCTGAT	TGCGGCAATTCGGACCTACGC
A_95_P015356	D86629	GGCAACGGAGGTGTTTCGGG	CCAGCCCCCGCGATCAAGCTG
A_95_P019246	FG638725	ATACAGAAATGCAGAAAATCCC	ACCAACTTATAAATGGAACAGAG
A_95_P020646	EB444675	TCAGGTGGTGTGGCGTAA	GCACATCATTAGACATCAGTTGGAA
A_95_P021466	EB445883	TTGGCTACTCTGTGTGCTAA	ACACATCTCCACCATCAAT
A_95_P027676	AF043554	GCTCTGAAGTTGGGTGTATGTG	TGGCATCGTTGGAGGACTC
A_95_P075770	BP526812	AGGTCCTTTGCTCAGCACGCA	TGGGACCCCAACAGCTCAAGT

Table 2-2. Primers used for qRT-PCR test (continuous)

Probe name	NCBI accession	Forward primer	Reverse Primer
A_95_P101828	EU123522	GCTGCTACGGTCTTTTGATCAGCCC	TGAAACGAGCCCCGAAGCTTGACA
A_95_P104722	CV015982	GTGTCCCAACAAGTTGTGTGTAGC	GCGGTGGCACAGCCTTTGTG
A_95_P112757	AB041519	CCCATCCAAAAGGCAAGTGCCCA	AGCAGCCTCAAGGTCAGCAACA
A_95_P114413	CV021588	AAGTTGTTACAGAAAGAGACCAT	GGGCTAAGGACCTCAAAAG
A_95_P115397	DV157577	CCCTGGTAGGCCCCACCCCTC	GCCAGGTGGCCTTGTGACCG
A_95_P121177	DW001196	TTACCGACTTGATAATATGACTT	AACCTCTCACCAACCAAAT
A_95_P129257	EB428960	AGAGGCAGGCATTGGAGACA	CGTTGGCATACTTGGTGGAGAC
A_95_P139897	EB443821	TCGGGGCTAAATTGCCCCAGCCA	ACGATGGTAACATGGTGCAAAGCC
A_95_P153957	EB684101	GCAGATGAGAAAGGTATTACAAGCA	GCGTAAGAAAGCATGAGCATGAATT
A_95_P160832	EH623698	CTCATCTCATATTTAGTCCCTCAA	CCACTACCCATATCGTTATACAA
A_95_P164222	EH623367	CCTCTACACTTCTCTCTGCCATAC	CCTCTCCAACACTCTCCACAA
A_95_P174692	EB450585	CCGCTAGCCCCCGCGATCAAG	GCAAGGCAGGTGCCCGAGAG
A_95_P176232	T18330	GCAGCAGCAAAAGGGATCGGC	CCGCCGGAGCTGTCGAGAAT

Table 2-2. Primers used for qRT-PCR test (continuous)

Probe name	NCBI accession	Forward primer	Reverse Primer
A_95_P202652	EB443656	AGTGTGAGGGCACAGGGAA	CTTGGCTGTAGGCGCCGAGG
A_95_P205197	BQ842956	GCCAGGTGGCCTTGTGACCG	CCCTGGTAGGCCCCACCCCTC
A_95_P218347	AB034638	TGCGATTAGAAGCGCGGTTGGT	TGAACCCGAGCCATCGACACA
A_95_P223717	FG636940	GCGACCAAGCAAAGGAAGA	CAAGATAAGCCAAGGGAATTACGA
A_95_P232164	BP128741	GTTCAAGCCTCATATTACAAA	GCTGTTCTCCAGACTGTT
A_95_P233804	FG137954	TTGGTTGTGGATAATTGTGGAA	CAGGTGGCAAGTTGATAGG
A_95_P244112	EB679225	ATGGTCACGGGAGAGATG	GCATAAGTTCAATCAGGTAAGGT
A_95_P248077	DW0033388	CACACAACTTGGGTTGGCTGAGT	GCCGTGAGTCCATCATCGCCC
A_95_P258416	GU994208	ACTATACTCCCTGACCTCTGTTT	ATTCCCTAATGCTGCTTCCAAGA
A_95_P260586	FG191218	GCTTCAAAGTTCCACAAAGTC	GTTCCCTCCAGTTACACCAT
A_95_P287758	FG152217	AGAGGCAGGCATTGGAGACA	GTTGGCATACTTGGCGGAGAC
A_95_P291753	EB424775	GCGGTTCCAATGACTATTATG	CTTGATCTAGGCGGTGTT
A_95_P306688	AB263747	GAGGGGTTCAAAGTTTCTAATTCT	CTCAACAGATAGCGGACAATG

Table 3-1. Numbers of differentially expressed genes analyzed by microarray.

Transcriptome comparison	Up-regulated*	Down-regulated*
HR DrolB vs. HR WT**	6	242
HR DrolC vs. HR WT**	42	208
HR DrolA vs. HR WT***	217	352
HR DrolD vs. HR WT***	271	297

* Genes were meshed under 2-fold cut off threshold

** Two biological replicates were performed in a dye-swap manner.

***Only one biological sample had been analyzed.



Table 3-2. GO term of down regulated genes in HR $\Delta rolB$ compared to HR WT.

GO term	<i>p</i> -value	FDR
lipid transport	1.80E-15	3.00E-13
lipid localization	3.10E-15	3.00E-13
lipid binding	2.80E-11	2.10E-09
macromolecule localization	1.70E-06	0.00011
response to wounding	2.80E-06	0.00014
hydrolase activity, hydrolyzing O-glycosyl compounds	7.30E-06	0.00028
hydrolase activity, acting on glycosyl bonds	2.60E-05	0.00066
endomembrane system	3.30E-05	0.0018
response to chemical stimulus	0.00018	0.0068
oxidoreductase activity, acting on peroxide as acceptor	0.00025	0.0038
peroxidase activity	0.00025	0.0038
response to stimulus	0.00026	0.008
response to stress	0.00029	0.008
response to external stimulus	0.0004	0.0095
electron carrier activity	0.0005	0.0064
antioxidant activity	0.00089	0.0097
extracellular region	0.00096	0.026
oxidoreductase activity	0.001	0.0097
lyase activity	0.0013	0.011
transport	0.0015	0.031
establishment of localization	0.0016	0.031
cation binding	0.002	0.014
ion binding	0.002	0.014
cellular amino acid derivative biosynthetic process	0.0021	0.034
localization	0.0022	0.034
response to endogenous stimulus	0.0023	0.034
oxidoreductase activity, acting on the CH-OH group of donors, NAD or NADP as acceptor	0.0026	0.017
response to hormone stimulus	0.0034	0.044
response to ethylene stimulus	0.0035	0.044
oxidoreductase activity, acting on CH-OH group of donors	0.0045	0.027
cellular amino acid derivative metabolic process	0.0067	0.08
response to organic substance	0.013	0.14
carbohydrate metabolic process	0.023	0.24
transition metal ion binding	0.03	0.16
metal ion binding	0.031	0.16

Table 3-3. GO analysis in terms of biological process of HR $\Delta rolB$ down regulated genes compared with those in HR WT.


Probe name	NCBI accession	GO source	Description	Microarray		qRT-PCR	
				Fold change	Fold	p-value	
Lipid transport							
A_95_P112757	AB041519	AT1G12090 1.00E-32	 lipid binding extensin-like protein (ELP)	0.2858	0.3653	0.0623	0.0010
A_95_P015356	D86629	AT1G12090 1.00E-33		0.3041	0.1956	0.0192	0.0010
A_95_P102367	AB041519	AT1G12090 5.00E-10		0.3024	0.3684	0.0623	0.0010
A_95_P174692	EB450585	AT1G12090 6.00E-12		0.2387	0.2298	NA	NA
A_95_P112022	AB041519	AT1G12090 9.00E-50		0.3038	0.4126	0.0623	0.0010
A_95_P115397	DV157577	AT1G62500 2.00E-72	protease inhibitor/seed storage/lipid transfer protein (LTP) family protein	0.2813	0.2694	NA	NA
A_95_P205197	BQ842956	AT1G62500 5.00E-76		0.2746	0.2984	0.0575	0.0010

Table 3-3. GO analysis in terms of biological process of HR $\Delta rolB$ down regulated genes compared with those in HR WT (continued)

Probe name	NCBI accession	GO source	Description	Microarray		qRT-PCR	
				Fold change		Fold	p-value
Lipid transport							
A_95_P027676	AF043554	AT1G62510 4.00E-32	protein_coding protease inhibitor/seed storage/lipid transfer protein (LTP) family protein	0.1805	0.1966	NA*	NA
A_95_P005446	AB035125	AT1G62510 4.00E-35		0.0432	0.0741	NA	NA
A_95_P000541	BQ842876	AT1G62510 5.00E-52		0.3738	0.3844	NA	NA
A_95_P004391	EH618856	AT1G62510 7.00E-50		0.3510	0.3523	0.0594	0.0010
A_95_P109177	D86629	AT3G22142 6.00E-14	structural constituent of cell wall Encodes a Protease inhibitor/seed storage/LTP family protein	0.2227	0.2197	0.0192	0.0010
A_95_P248077	DW003388	AT5G48485 6.00E-21	DIR1 (DEFECTIVE IN INDUCED RESISTANCE 1)	0.2299	0.3427	0.0268	0.0020
A_95_P202652	EB443656	AT5G48485 7.00E-22		0.1074	0.1052	0.0495	0.0010
Cellular amino acid derivative biosynthetic process							
A_95_P029796**	AB012857	AT1G05010 8.00E-57	EFE (ETHYLENE-FORMING ENZYME); 1-aminocyclopropane-1-carboxylate oxidase (ACO)	0.2937	0.4772		
A_95_P122162	DW002203	AT1G16490 2.00E-26	MYB DOMAIN PROTEIN 58 (MYB58)	0.3608	0.3718		

Table 3-3. GO analysis in terms of biological process of HR $\Delta rolB$ down regulated genes compared with those in HR WT (continued)

Probe name	NCBI accession	GO source	Description	Microarray		qRT-PCR	
				Fold change		Fold	p-value
Cellular amino acid derivative biosynthetic process							
A_95_P218347	AB034638	AT2G02990 8.00E-92	RNS1 (RIBONUCLEASE 1)	0.3273	0.4216	0.2120	0.0010
A_95_P293088	AB176525	AT3G29590 3.00E-33	AT5MAT; O-malonyltransferase/ transferase At3g29590 (At5MAT)	0.3551	0.4881	NA	NA
A_95_P283463	EU123523	AT3G49700 1.00E-113	ACS9 (1-AMINOCYCLOPROPANE-1-CARBOXYLATE SYNTHASE 9)	0.4198	0.4460		
A_95_P101828	EU123522	AT4G11280 2.00E-67	ACS6 (1-AMINOCYCLOPROPANE-1-CARBOXYLIC ACID (ACC) SYNTHASE 6)	0.3768	0.4916	0.2976	0.0010
Response to wounding							
A_95_P218347	AB034638	AT2G02990 8.00E-92	RNS1 (RIBONUCLEASE 1)	0.3273	0.4216	0.2120	0.0010
A_95_P010771	X51426	AT3G12500 4.00E-81	ATHCHIB (ARABIDOPSIS THALIANA BASIC CHITINASE)	0.2679	0.3354	0.2183	0.0010
A_95_P104722	CV015982	AT3G12500 5.00E-13		0.1019	0.2023	0.0260	0.0010
A_95_P114413	CV021588	AT4G10265 2.00E-12	putative wound-responsive protein	0.0532	0.3944	NA	NA

Table 3-3. GO analysis in terms of biological process of HR $\Delta rolB$ down regulated genes compared with those in HR WT (continued)


Probe name	NCBI accession	GO source	Description	Microarray		qRT-PCR	
				Fold change	Fold	p-value	
Response to wounding							
A_95_P176232	T18330	AT4G10270 1.00E-15	 wound-responsive family protein	0.2287	0.3635	0.0881	0.0010
A_95_P139897	EB443821	AT4G10270 2.00E-21		0.1830	0.3192	0.0592	0.0010
A_95_P003336	DR752062	AT4G10270 2.00E-22		0.1291	0.2231	0.0463	0.0010
A_95_P075770	BP526812	AT4G10270 3.00E-25		0.2589	0.2429	0.0784	0.0010
A_95_P101828	EU123522	AT4G11280 2.00E-67		0.3768	0.4916	0.2976	0.0010
Response to ethylene stimulus							
A_95_P020646	EB444675	AT2G14580 2.00E-53	ATPRB1 pathogenesis related protein, encodes a basic PR1-like protein	0.2168	0.2019	NA	NA

Table 3-3. GO analysis in terms of biological process of HR $\Delta rolB$ down regulated genes compared with those in HR WT (continued)

Probe name	NCBI accession	GO source	Description	Microarray		qRT-PCR	
				Fold change	Fold	p-value	
Response to ethylene stimulus							
A_95_P110557	CV015982	AT3G04720 3.00E-12	PR4 (PATHOGENESIS-RELATED 4)	0.1433	0.1929	0.0260	0.0010
A_95_P010771	X51426	AT3G12500 4.00E-81	ATHCHIB (ARABIDOPSIS THALIANA BASIC CHITINASE)	0.2679	0.3354	0.2183	0.0010
A_95_P104722	CV015982	AT3G12500 5.00E-13		0.1019	0.2023	0.0260	0.0010
A_95_P101828	EU123522	AT4G11280 2.00E-67	ACS6 (1-AMINOCYCLOPROPANE-1-CARBOXYLIC ACID (ACC) SYNTHASE 6)	0.3768	0.4916	0.2976	0.0010

* NA represent no qRT-PCR data available

** Dark background represent probes without appropriate NCBI accession

Table 3-4. GO results of HR $\Delta rolC$ down regulated genes compared to HR WT.

Term	<i>p</i>-value	FDR
lipid transport	6.00E-12	6.40E-10
lipid localization	9.10E-12	6.40E-10
macromolecule localization	5.20E-05	0.0024
response to chemical stimulus	0.00019	0.0041
localization	0.00022	0.0041
transport	0.00014	0.0041
establishment of localization	0.00015	0.0041
response to stimulus	0.00023	0.0041
response to wounding	0.00052	0.0081
carbohydrate metabolic process	0.0011	0.015
ion transport	0.0063	0.075
response to metal ion	0.0064	0.075
response to inorganic substance	0.0095	0.1
response to stress	0.012	0.11
response to external stimulus	0.012	0.11
response to hormone stimulus	0.011	0.11
response to endogenous stimulus	0.018	0.15

Table 3-5. GO analysis in terms of biological process of HR $\Delta rolC$ down regulated genes compared with those in HR WT.

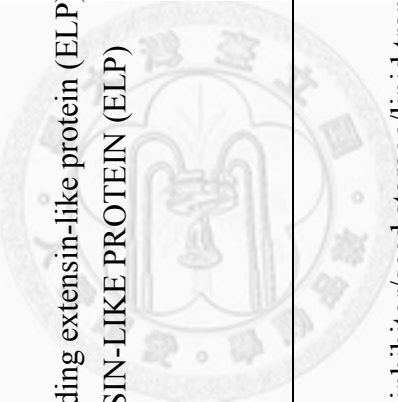
Probe name	NCBI accession	GO source	Description	Microarray		qRT-PCR	
				Fold change	Fold	p-value	
Lipid transport							
A_95_P112757	AB041519	AT1G12090	 lipid binding extensin-like protein (ELP)	0.3996	0.2092	0.3602	0.0010
		1.00E-32					
A_95_P015356	D86629	AT1G12090		0.4105	0.2662	0.3602	0.0010
		1.00E-33					
A_95_P112022	AB041519	AT1G12090		0.3770	0.1774	0.2479	0.0010
		9.00E-50					
A_95_P115397	DV157577	AT1G62500		0.1461	0.0072	0.1254	0.0010
		2.00E-72					
A_95_P205197	BQ842956	AT1G62500		0.3576	0.0685	0.1642	0.0010
		5.00E-76					
A_95_P027676	AF043554	AT1G62510	0.3576	0.0685	0.1642	0.0010	
		4.00E-32					protein protease inhibitor/seed storage/lipid transfer protein (LTP) family protein
A_95_P005446	AB035125	AT1G62510	0.3576	0.0685	0.1642	0.0010	
		4.00E-35					protein protease inhibitor/seed storage/lipid transfer protein (LTP) family protein

Table 3-5. GO analysis in terms of biological process of HR $\Delta rolC$ down regulated genes compared with those in HR WT (continued)

Probe name	NCBI accession	GO source	Description	Microarray		qRT-PCR	
				Fold change		Fold	p-value
Lipid transport							
A_95_P260586	FG191218	AT2G10940	protease inhibitor/seed storage/lipid transfer protein (LTP) family protein	0.4515	0.3719	0.5521	0.0010
		2.00E-54					
A_95_P233804	FG137954	AT3G22142	constituent of cell wall Encodes a Protease inhibitor/seed storage/LTP family protein	0.4378	0.4030	1.0033	0.0010
		3.00E-66					
A_95_P109177	D86629	AT3G22142	storage/LTP family protein	0.3384	0.0865	0.1946	0.0010
		6.00E-14					
A_95_P248077	DW003388	AT5G48485	DIR1 (DEFECTIVE IN INDUCED RESISTANCE 1); lipid binding	0.3560	0.3192	0.1077	0.0010
		6.00E-21					
Carbohydrate metabolic process							
A_95_P129257	EB428960	AT1G10640	polygalacturonase polygalacturonase	0.2664	0.2151	0.2927	0.0010
		2.00E-80					
A_95_P121177	DW001196	AT1G48100	glycoside hydrolase family 28 protein / polygalacturonase (pectinase) family protein	0.4150	0.4876	NA*	NA
		8.00E-88					
A_95_P287758	FG152217	AT1G60590	polygalacturonase, putative / pectinase, putative polygalacturonase	0.3404	0.1914	0.3002	0.0010
		4.00E-77					
A_95_P244112	EB679225	AT3G61490	glycoside hydrolase family 28 protein / polygalacturonase (pectinase) family protein	0.4459	0.4358	0.4036	0.0450
		1.00E-148					
A_95_P290538**		AT4G37800	xyloglucan:xyloglucosyl transferase, putative	0.3582	0.0943		
		1.00E-88					

Table 3-5. GO analysis in terms of biological process of HR $\Delta rolC$ down regulated genes compared with those in HR WT (continued)

Probe name	NCBI accession	GO source	Description	Microarray		qRT-PCR	
				Fold change		Fold	p-value
Carbohydrate metabolic process							
A_95_P030516		AT5G24090	acidic endochitinase (CHIB1) acidic endochitinase (CHIB1)	0.4277	0.4273		
		1.00E-105					
A_95_P159427		AT5G24090		0.3906	0.142		
		1.00E-66					
A_95_P013991		AT5G24090		0.4249	0.1557		
		4.00E-93					
A_95_P153957	EB684101	AT5G55180	glycosyl hydrolase family 17 protein	0.4091	0.3779	0.9363	0.0679
		1.00E-17					
A_95_P291753	EB424775	AT5G64570	XYL4; hydrolase, hydrolyzing O-glycosyl compounds / xylan 1,4-beta-xylosidase	0.4723	0.3989	NA	NA
		1.00E-101					
Response to chemical stimulus							
A_95_P258416	GU994208	AT1G07400	17.8 kDa class I heat shock protein (HSP17.8-CI)	0.4281	0.3861	NA	NA
		3.00E-59					
A_95_P223717	FG636940	AT1G29450	putative auxin-responsive protein	0.2947	0.432	0.898	0.1568
		8.00E-31					
A_95_P105042		AT1G76100	PETE1 (PLASTOCYANIN 1); copper ion binding / electron carrier One of two Arabidopsis plastocyanin genes	0.2515	0.1085		
		1.00E-59					
		AT1G76100		0.2724	0.1921		
A_95_P111392		3.00E-42					


Table 3-5. GO analysis in terms of biological process of HR $\Delta rolC$ down regulated genes compared with those in HR WT (continued)

Probe name	NCBI accession	GO source	Description	Microarray		qRT-PCR	
				Fold change	Fold	p-value	
Response to chemical stimulus							
A_95_P113472		AT1G76100	PETE1 (PLASTOCYANIN 1); copper ion binding / electron carrier One of two Arabidopsis plastocyanin genes	0.2695	0.1151		
		7.00E-37					
A_95_P109467		AT1G76100		0.4193	0.2264		
		7.00E-44					
A_95_P164222	EH623367	AT1G77120	ADH1 (ALCOHOL DEHYDROGENASE 1)	0.301	0.1121	NA	NA
		1.00E-106					
A_95_P144057		AT1G77120		0.301	0.1091	NA	NA
		3.00E-46					
A_95_P020646	EB444675	AT2G14580	ATPRB1 pathogenesis related protein, encodes a basic PR1-like protein	0.444	0.0405	0.1797	0.001
		2.00E-53					
A_95_P110557	CV015982	AT3G04720	PR4 (PATHOGENESIS-RELATED 4)	0.473	0.1023	0.161	0.001
		3.00E-12					
A_95_P104722	CV015982	AT3G12500	ATHCHIB (ARABIDOPSIS THALIANA BASIC CHITINASE)	0.3992	0.0937	0.161	0.001
		5.00E-13					
A_95_P232164	BP128741	AT3G56240	CCH (COPPER CHAPERONE)	0.3879	0.4368	NA	NA
		7.00E-30					

Table 3-5. GO analysis in terms of biological process of HR $\Delta rolC$ down regulated genes compared with those in HR WT (continued)

Probe name	NCBI accession	GO source	Description	Microarray		qRT-PCR	
				Fold change		Fold	p-value
Response to chemical stimulus							
A_95_P101828	EU123522	AT4G11280 2.00E-67	ACS6 (1-AMINOCYCLOPROPANE-1-CARBOXYLIC ACID (ACC) SYNTHASE 6);	0.4854	0.4895	0.3695	0.001
A_95_P021466	EB445883	AT4G17260 1.00E-104	putative L-lactate dehydrogenase	0.3277	0.182	0.4959	0.001
A_95_P158992		AT4G17260 2.00E-41		0.3632	0.2865	0.4959	0.001
A_95_P003626	FG637828	AT5G06730 5.00E-34	putative peroxidase	0.2812	0.2957	0.1847	0.001
A_95_P306688	AB263747	AT5G24380 3.00E-51	YSL2 (YELLOW STRIPE LIKE 2)	0.4	0.2218	0.8341	0.001
A_95_P160832	EH623698	AT5G53590 4.00E-22	auxin-responsive family protein	0.3634	0.2717	NA	NA
A_95_P007251	EF051128	AT5G54960 0	PDC2 (pyruvate decarboxylase-2)	0.4321	0.3272	0.3161	0.001
A_95_P019246	FG638725	AT5G59845 1.00E-27	gibberellin-regulated family protein gibberellin-regulated family protein	0.3765	0.3272	0.0924	0.001
A_95_P293048		AT5G65730 2.00E-93	xyloglucan:xyloglucosyl transferase, putative	0.4726	0.2793		

Table 3-5. GO analysis in terms of biological process of HR $\Delta rolC$ down regulated genes compared with those in HR WT (continued)

Probe name	NCBI accession	GO source	Description	Microarray		qRT-PCR	
				Fold change	Fold	p-value	
Response to wounding							
A_95_P104722	X51426	AT3G12500	ATHCHIB (ARABIDOPSIS THALIANA BASIC CHITINASE)	0.3992	0.0937	0.4414	0.001
		5.00E-13					
A_95_P101828	EU123522	AT4G11280	ACS6 (1-AMINOCYCLOPROPANE-1-CARBOXYLIC ACID (ACC) SYNTHASE 6)	0.4854	0.4895	0.3695	0.001
		2.00E-67					
A_95_P176232	T18330	AT4G10270	 wound-responsive family protein wound-responsive family protein	0.2978	0.2474	0.2237	0.001
		1.00E-15					
AT4G10270	0.2796	0.1598		0.2953	0.001		
3.00E-25							
A_95_P003336	DR752062	AT4G10270		0.1692	0.1413	0.0583	0.001
		2.00E-22					
A_95_P139897	EB443821	AT4G10270		0.2516	0.2476	0.3185	0.001
		2.00E-21					

* NA represent no qRT-PCR data available

** Dark background represent probes without appropriate NCBI accession

Figures

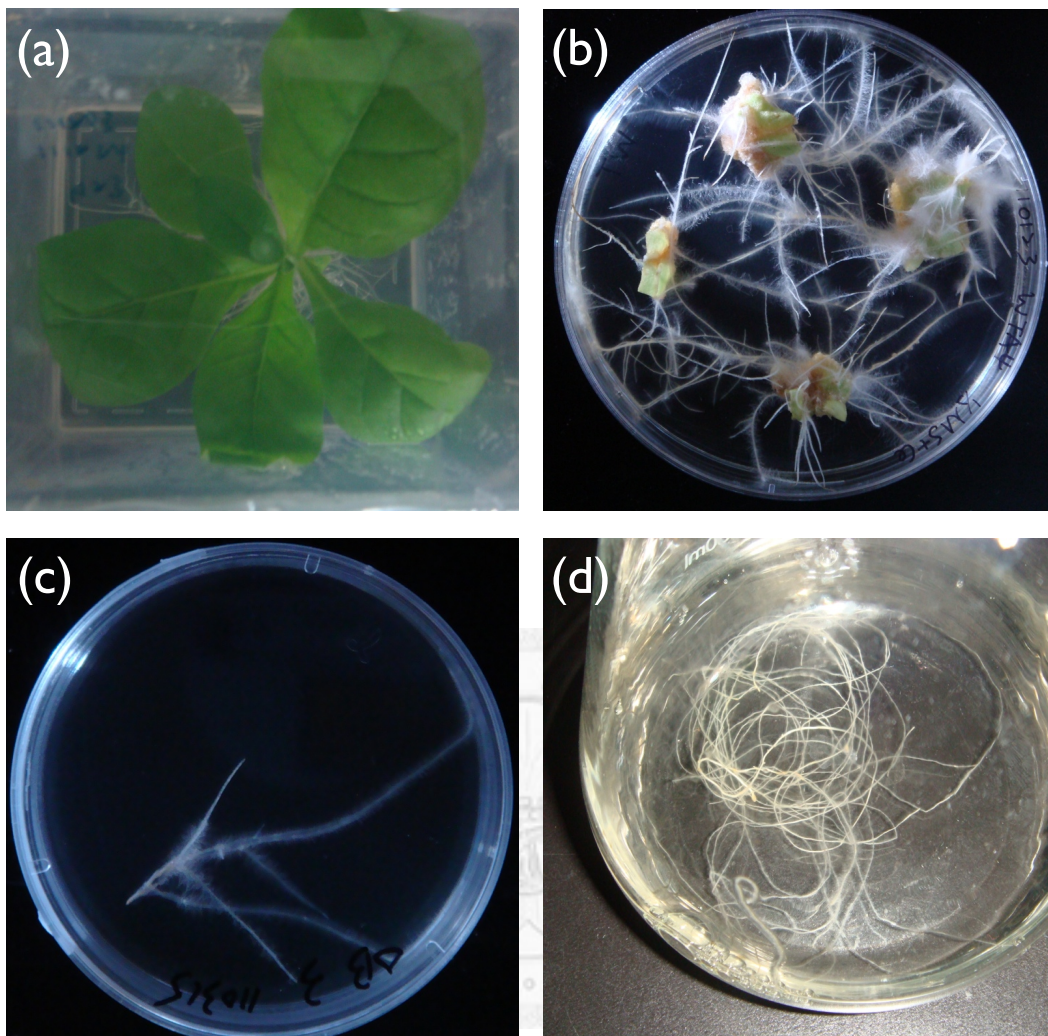


Figure 1-1. Hairy root.

After *A. rhizogenes* infecting healthy 8-week-old tobacco leaf discs (a), hairy roots start to emerge from the infecting site (b). Each hairy root can be cultured independently in solid (c) or liquid (d) phytohormone-free medium. Images provided by Jung-Hao Wang, unpublished data.

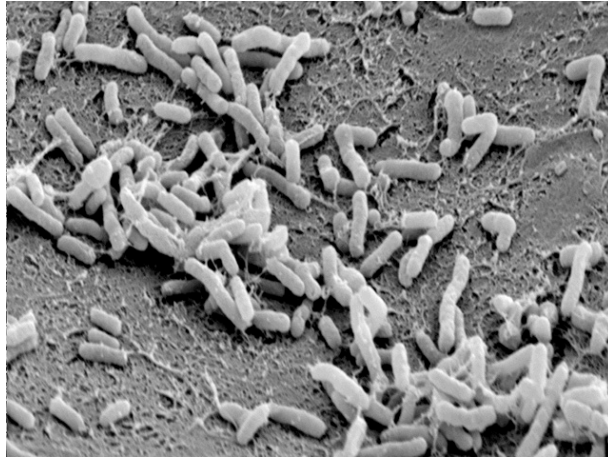


Figure 1-2. *A. rhizogenes* under microscope.

A. rhizogenes is a rod-shape, gram-negative soil bacterium. It can infect plant cell and transform it into hair root. Image retrieved from:

<http://commtechlab.msu.edu/sites/dlc-me/zoo/microbes/agrobacterium.html>



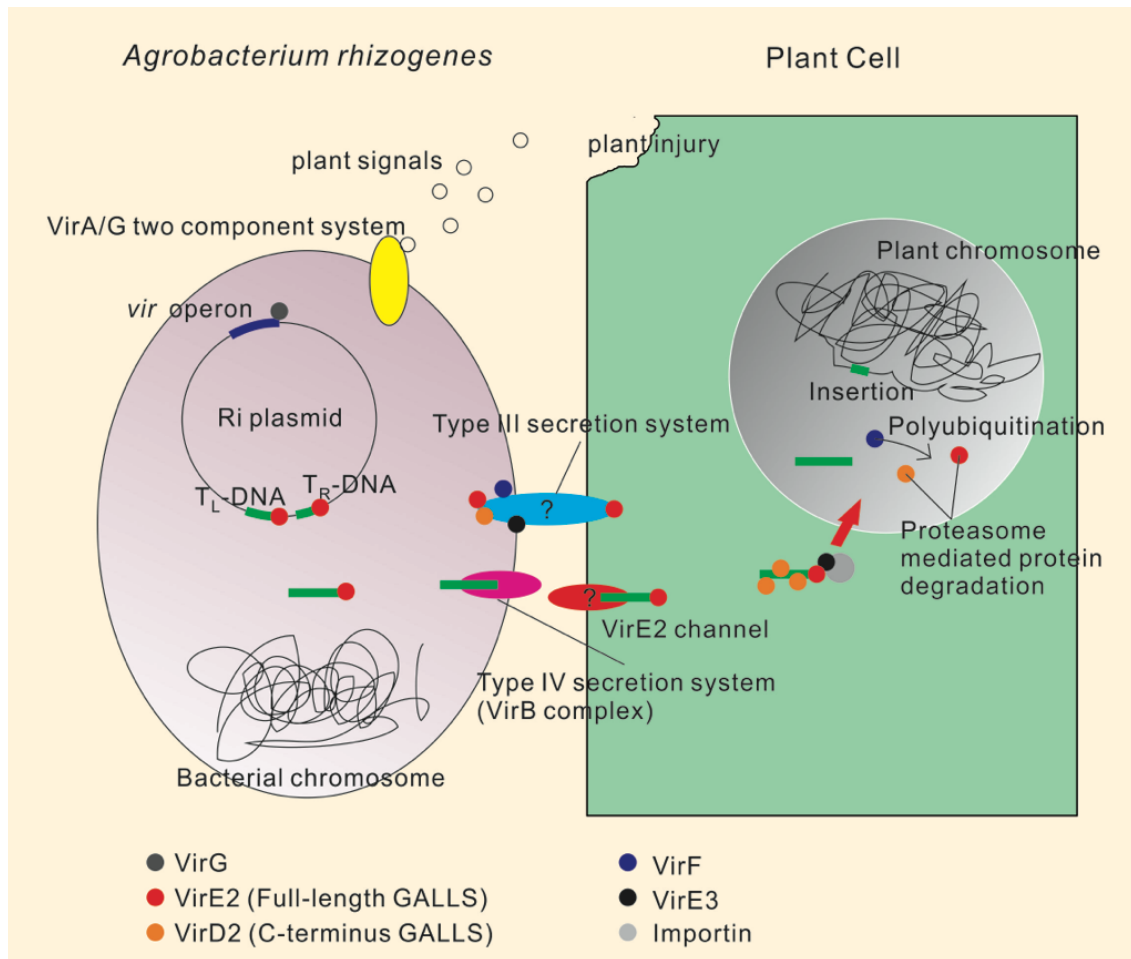


Figure 1-3. Molecular mechanisms of how *A. rhizogenes* infects plant cell.

Phenolic compound (open circle) will be released as a plant signals after plant injury. This signal can be sensed by the VirA/G two component systems (yellow circle) of *A. rhizogenes*, and resulted in T-DNA (green bar) transform and insert into plant nucleus. The expression of the inserted T-DNA will transformed the plant cell into hairy root morphology. Image provided by Jung-Hao Wang, unpublished.

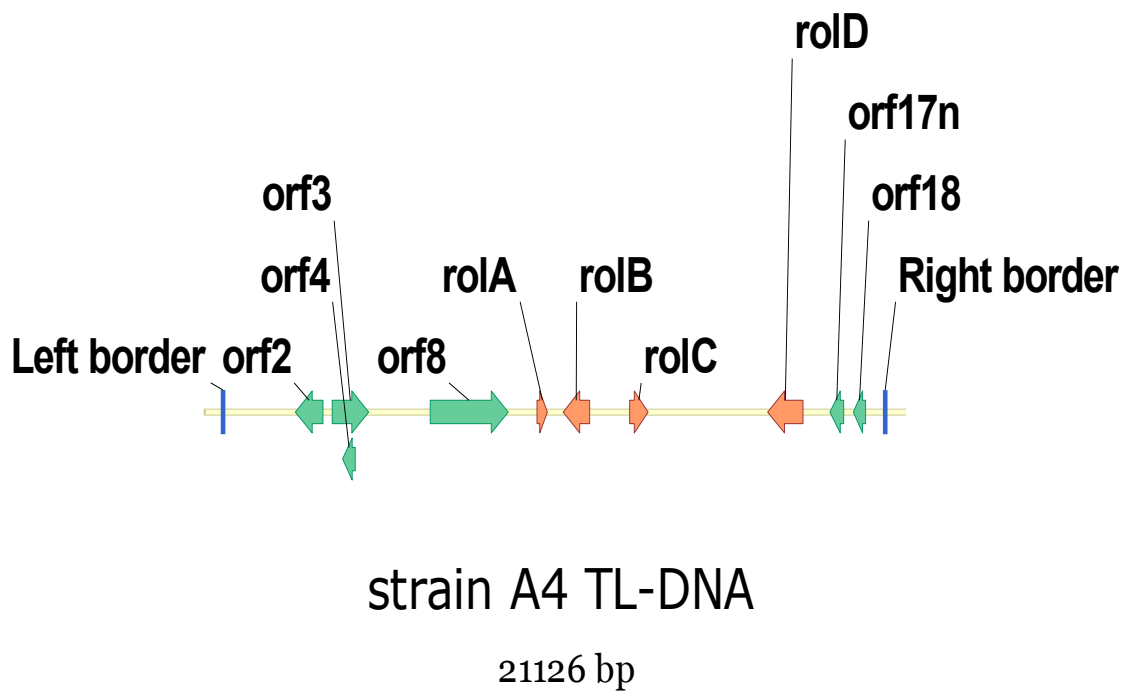


Figure 1-4. The TL-DNA region of *A. rhizogenes* strain A4.

The *rol* genes are shown in orange arrows while the other open reading frames (ORFs) are shown in green. The left and right borders are shown in blue lines. NCBI accession number K03313.



Figure 2-1. Target region of the pK18HRrol check primers.

Blue line indicated the individual *rol* genes, and the red arrow indicated the forward and reverse of pK18HRrol check primer. Therefore, PCR fragment of deleted *rol* gene should have PCR product smaller than that of the wild type.





Figure 2-2. Measuring hairy root architecture.

The hairy root elongate from the sub-cultured 1.5 cm hairy root tip was defined as the main root (dash line). Branch root was defined as the roots directly protrude from the main root (asterisk). Total branch root length was defined as the total length of branch root. Branch root density was defined as the branch number per cm of main root (cm^{-1}).

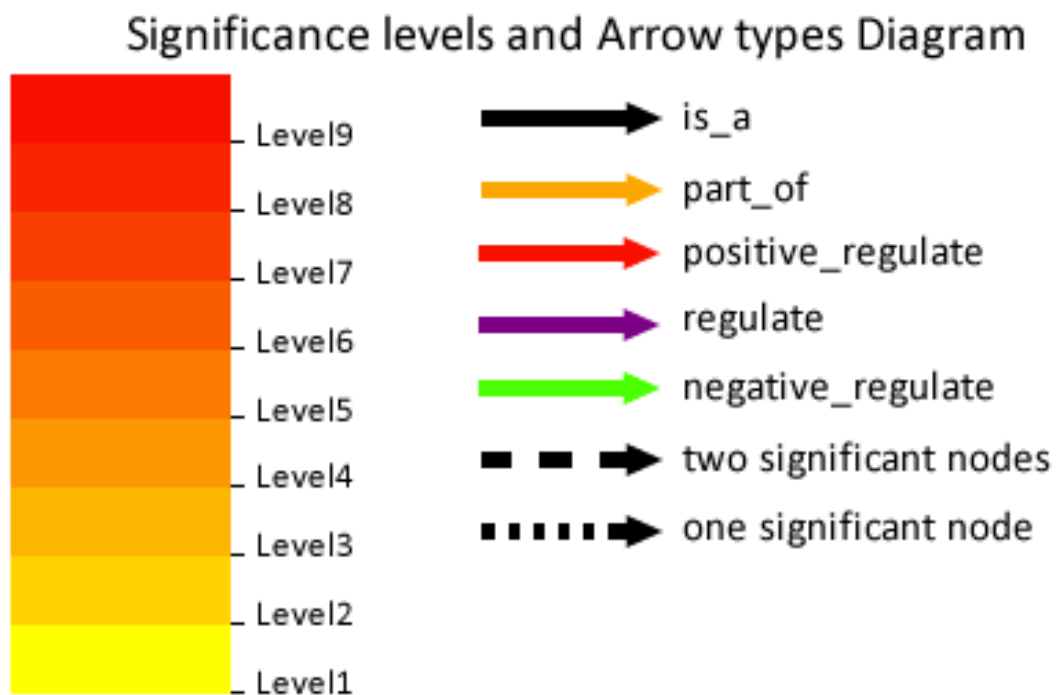


Figure 2-3. Explanation of Gene Ontology diagram.

The left column demonstrate the ten level of significant differences expressed by color in the block. The right column demonstrates the types of arrows used in the diagram.

Retrieved from: <http://bioinfo.cau.edu.cn/agriGO/graphresult.php>

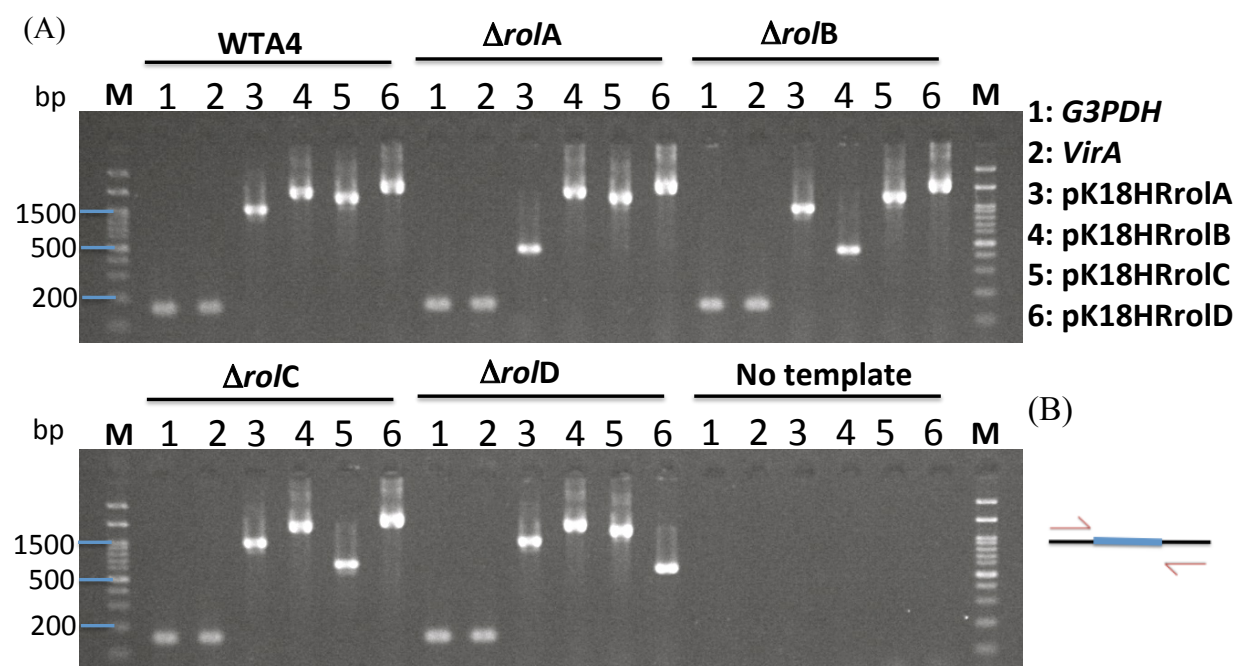


Figure 3-1. Genotype confirmation of *A. rhizogenes* strain A4 and its derivatives.

Ten ng of genomic DNA of *A. rhizogenes* strain A4 and its derivatives were used as the templates for amplification using the following primers: *G3PDH*, *VirA*, pK18HRrolA check, pK18HRrolB check, pK18HRrolC check, and pK18HRrolD check. The primer designation is shown in (B) where blue line indicated the gene to be deleted, and the red arrow indicated the forward and reverse of pK18HRrol check primer. Therefore, PCR fragment of deleted *rol* gene should have PCR product smaller than that of the wild type, as shown in (A). For example, $\Delta rolA$ has corresponding pK18rolA product of smaller size than that of wild type. *g3pdh* and *virA* served as a bacterium control and Root inducing plasmid (pRi) control, respectively. Water was added instead of DNA in no template group.

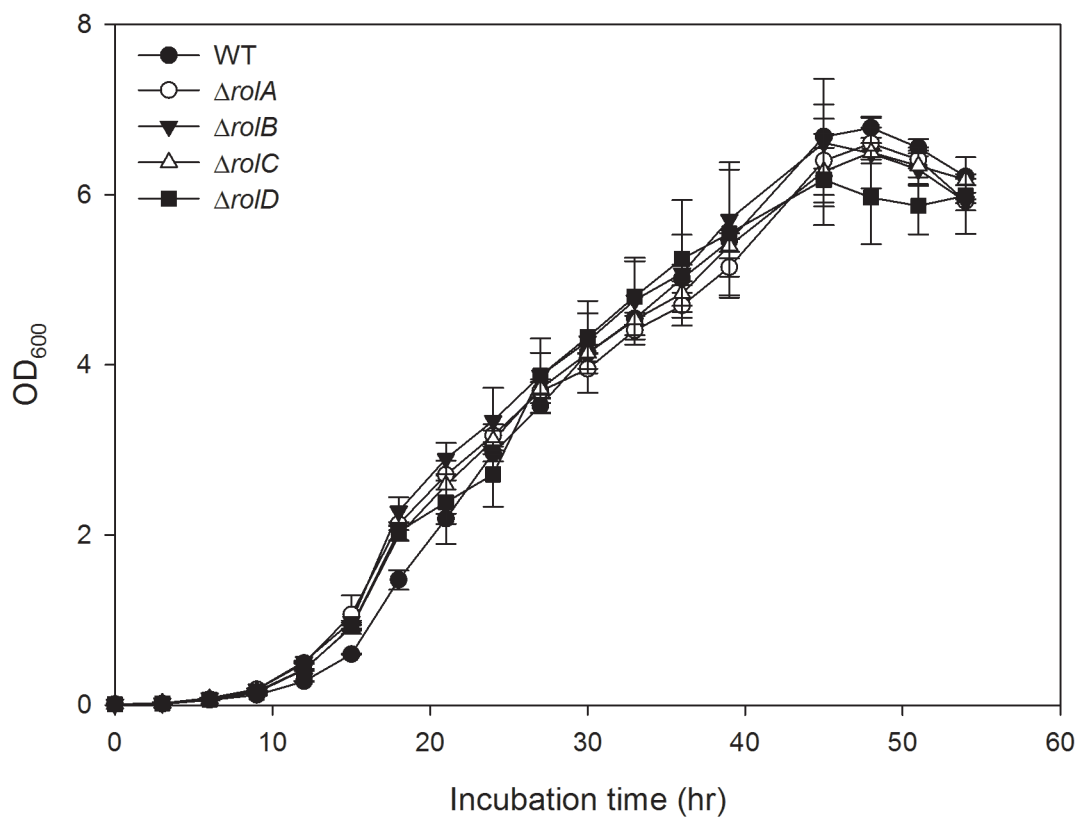


Figure 3-2. Growth curve of wild type and the *rol* gene-deficient *A. rhizogenes* strain A4.

OD₆₀₀ were recorded every 3 hours after inoculation. Three biological replicates were performed in each group. The results showed that wild type *A. rhizogenes* strain A4 grew slower than its *rol* gene-deficient derivatives during 12-24 h after inoculation. However, there was no significant differences between all groups when incubated longer than 24 h. All genotypes reached stationary phase at about 48 h.

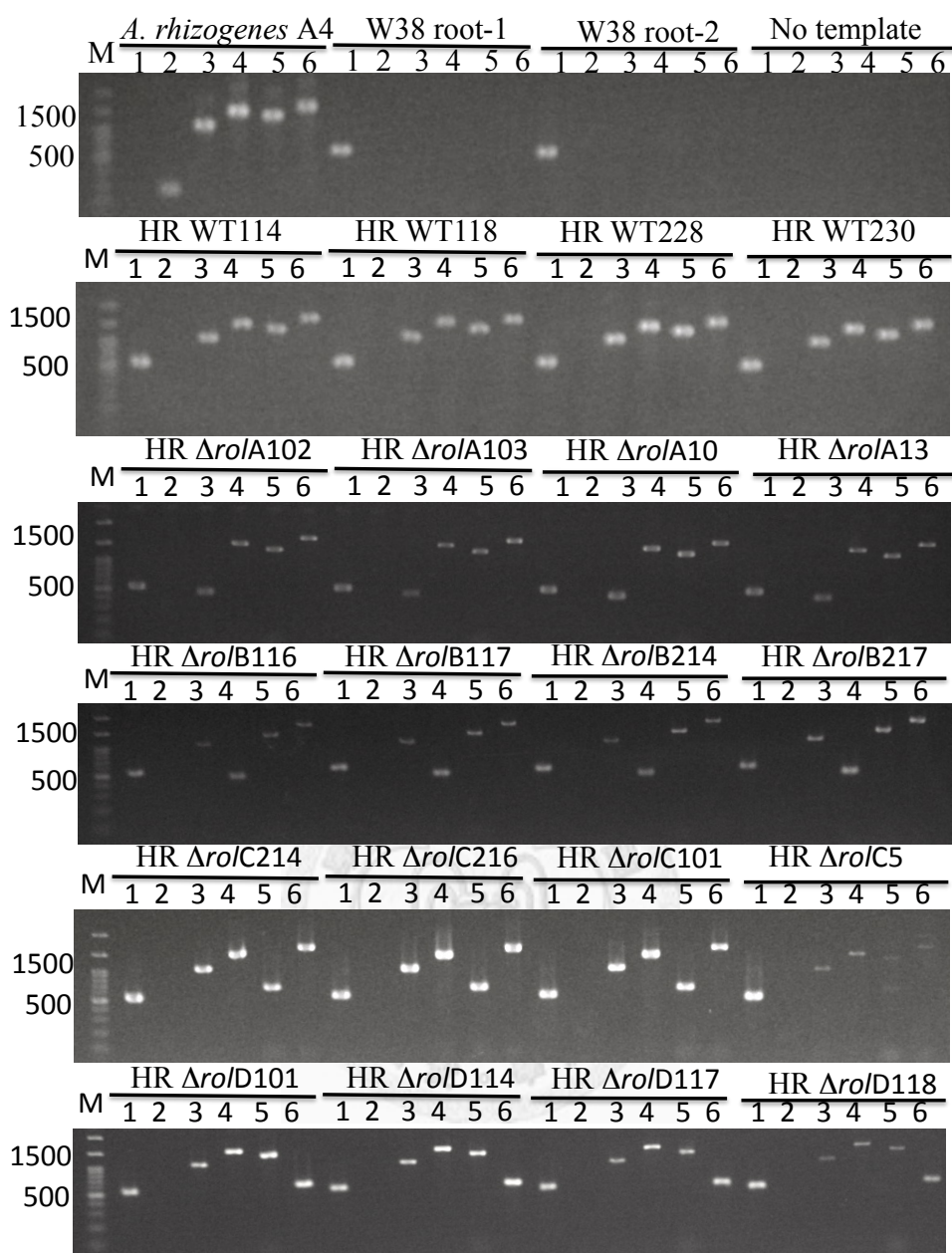


Figure 3-3. Confirmation of hairy root genotype.

Hairy root genotype was confirmed using chromosome DNA by pK18HRrol primers. In each genotype of hairy root, four independent clones are shown here as a representative data. *A. rhizogenes* A4 served as a positive control of full length *rol* genes, while W38 served as a negative control. No template, on the other hand, served as a negative reagent control. The numbers of each primer were 1: tobacco *ACTIN-9*, 2: *VirA*, 3: pK18HRrolA, 4: pK18HRrolB, 5: pK18HRrolC, 6: pK18HRrolD.

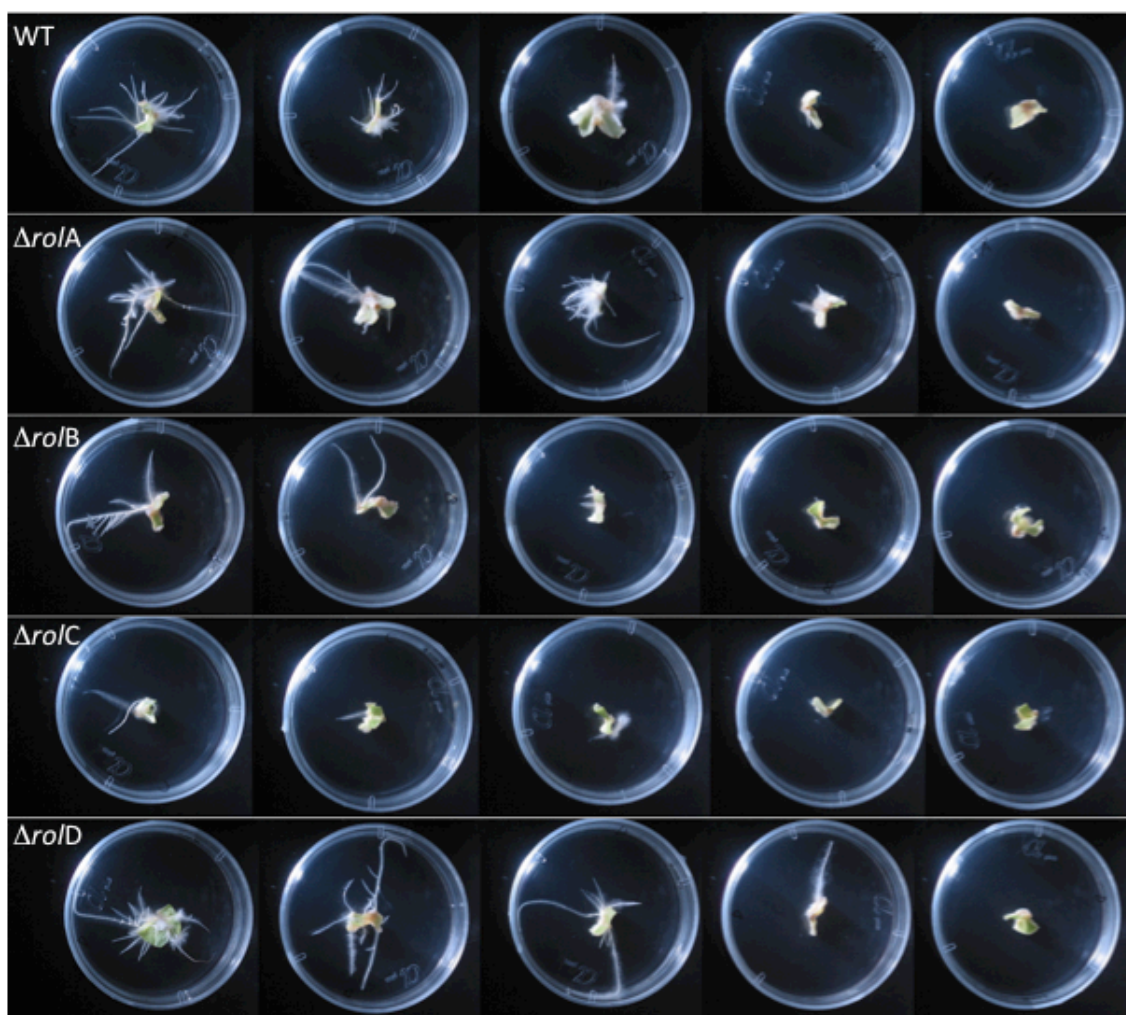


Figure 3-4. Phenotypes of *A. rhizogenes* A4 and its derivatives-infected tobacco leaf discs at 21 dpi.

Thirty independent leaf discs were infected in each group. Systematic sampling chosen-leaf discs are shown. Hairy root numbers were less in $\Delta rolB$ - and $\Delta rolC$ -induced leaf discs than WTA4-induced ones. Moreover, hairy root length in $\Delta rolB$ - and $\Delta rolC$ -induced leaf discs were also shorter, indicated that $\Delta rolB$ and $\Delta rolC$ were less virulent.

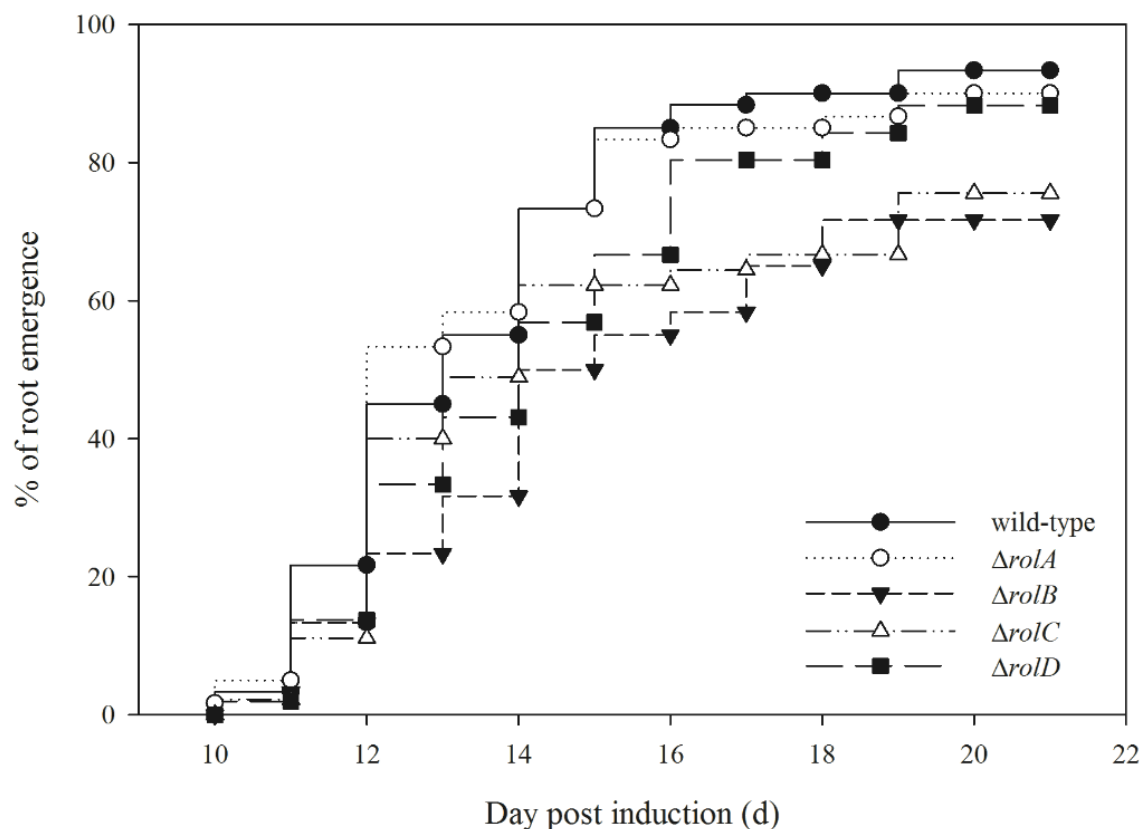


Figure 3-5. Days to the first root emergence post induction (DREPI).

The hairy root inducing rate of $\Delta rolB$ and $\Delta rolC$ were significant lower than that of the WT A4 ($p = 1.1 \times 10^{-3}$, and 8.4×10^{-6} , respectively). On the other hand, although $\Delta rolD$ has lower root emergence rate before 16 dpi, the emergence rate at 21 dpi shows no significant differences than that of WT A4 ($p = 1.0$). Significant differences test were performed using Mann-Whitney U test adjusted with Bonferroni correction. The number of replications in each group was 60, 60, 60, 45, and 52, respectively.

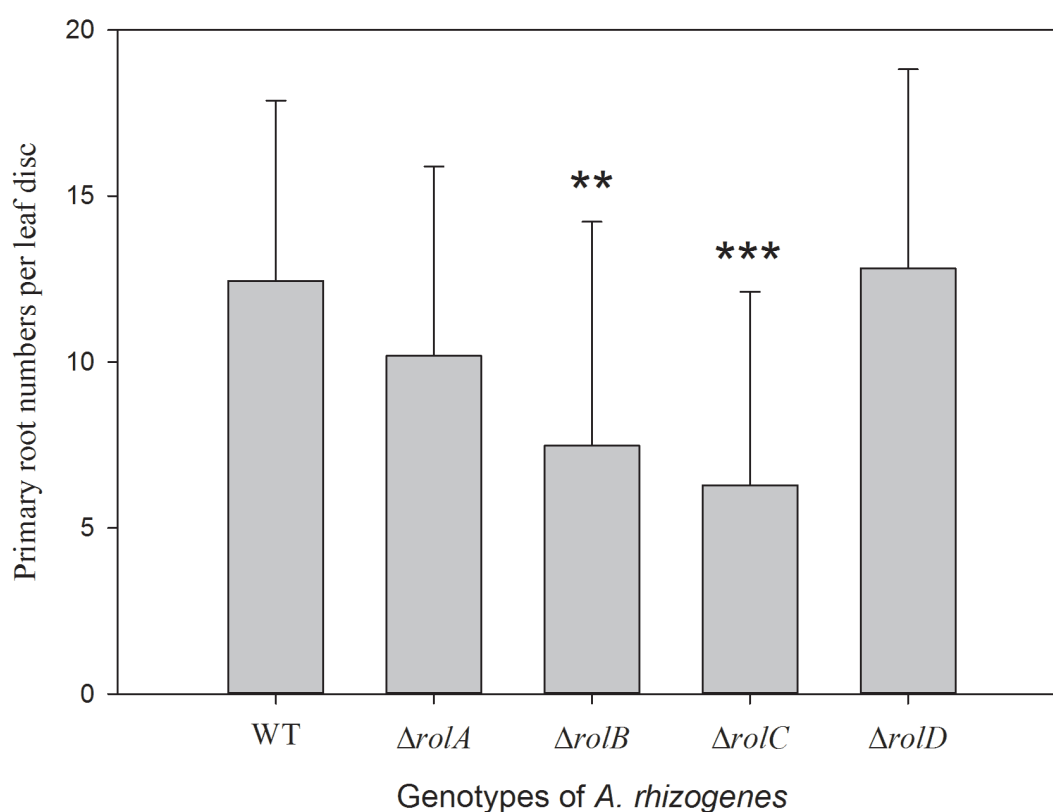


Figure 3-6. Primary root number per leaf disc (RL ratio) at 21 dpi.

Hairy root number induced by *A. rhizogenes* strain A4 and its derivatives were recorded. The bar represents the mean and the error bar represents the standard deviation. Significant differences test using Mann-Whitney U test adjusted with Bonferroni correction revealed significant differences existed between WTA4 and $\Delta rolB$ and between WTA4 and $\Delta rolC$. The number of replications in each group was 60, 60, 60, 45, and 52, respectively. (** $p < 0.01$, *** $p < 0.001$).

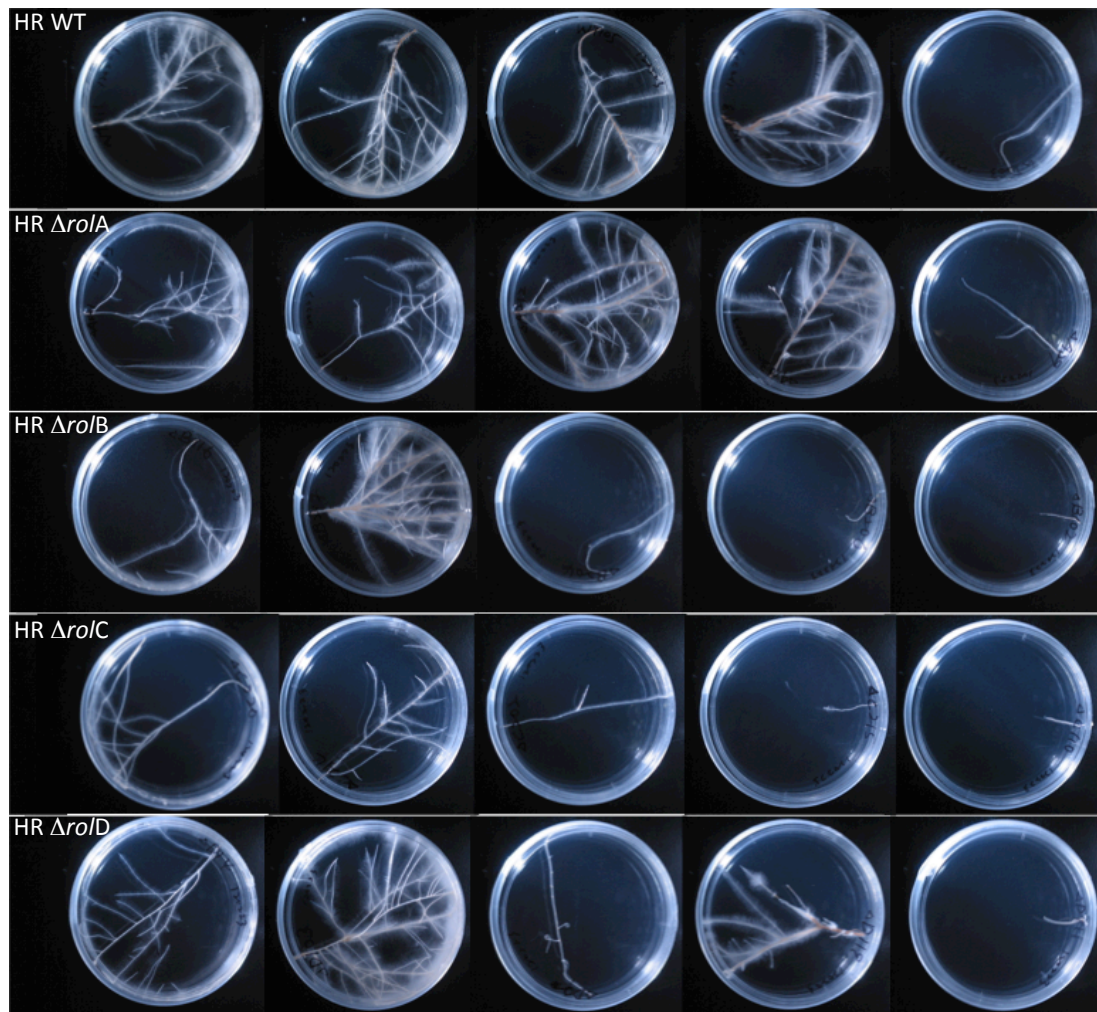


Figure 3-7. Selected hairy root appearances after 18 days post sub-culturing.

The hairy roots were selected systematically according to their main root length. Each row represents a specific genotype. The population of HR $\Delta rolB$ and $\Delta rolC$ groups seems to show shorter main root length and retard branch root system. The independent clones observed in HR WT, HR $\Delta rolA$, HR $\Delta rolB$, HR $\Delta rolC$, and HR $\Delta rolD$, were 84,93,65,82, and 58.

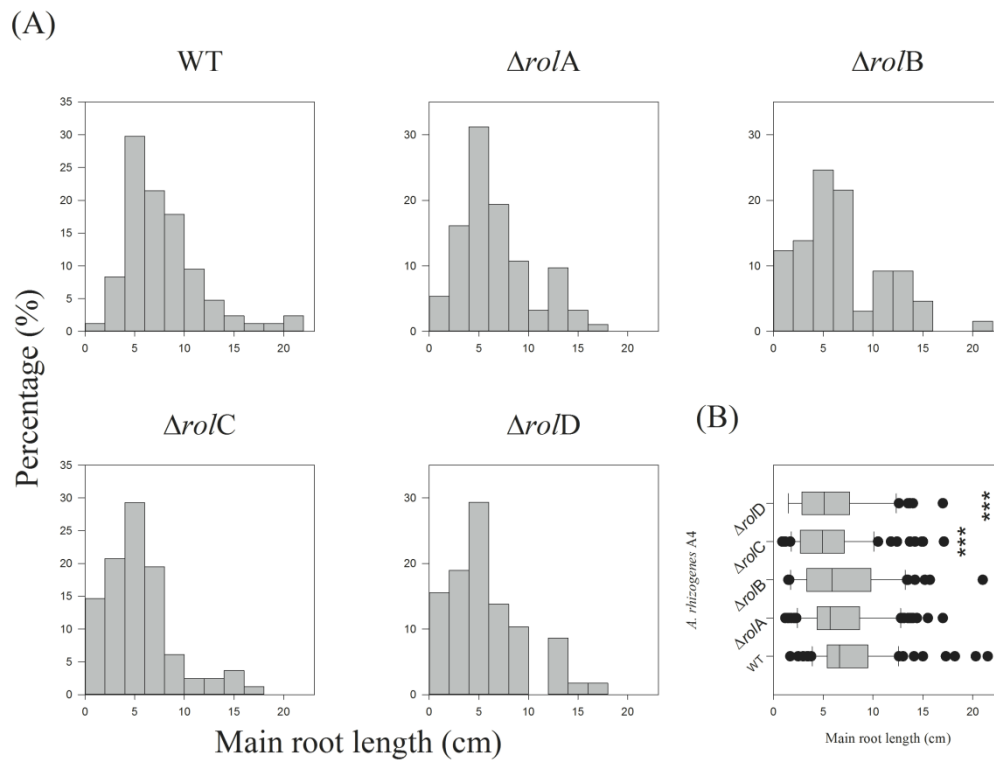


Figure 3-8. Main root length of *A. rhizogenes* A4 and its *rol* gene-deficient derivatives.

Population distribution of each groups are shown in (A). Main root length is shown in x-axis while percentage of the population shown in y-axis. Box plot of each group are shown in (B) where the dots represent the outliers. Significant differences were analyzed using permutation by ANOVA with 1000 replications against HR WT. (***) $p < 0.001$).

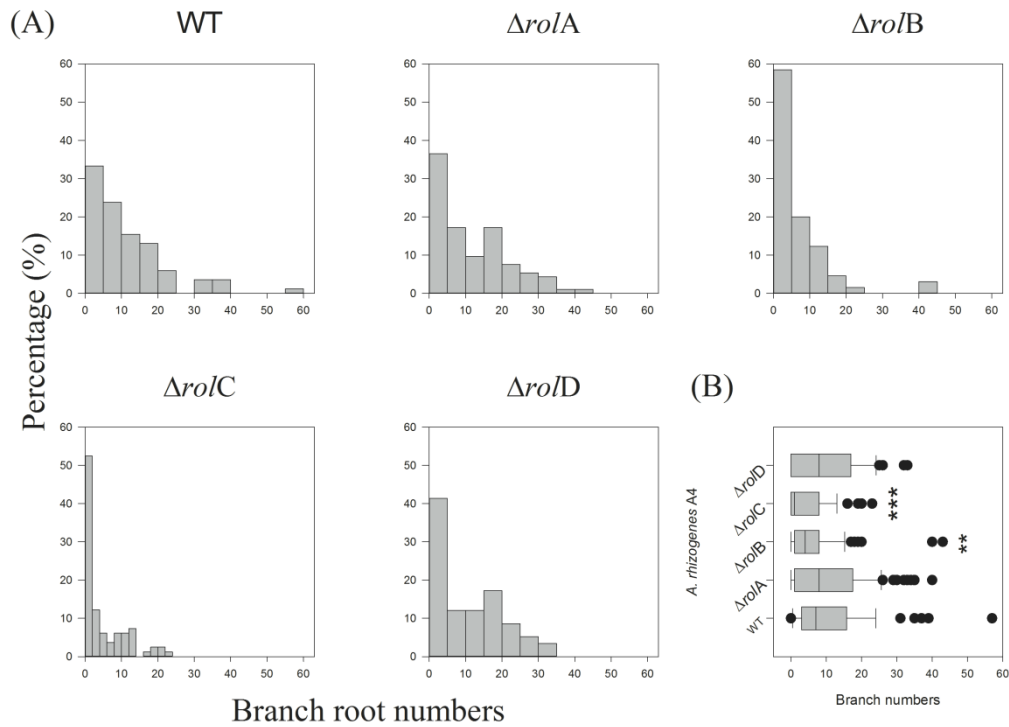


Figure 3-9. Branch root number of *A. rhizogenes* A4 and its *rol* gene-deficient derivatives.

Population distribution of each groups are shown in (A). Branch root number is shown in x-axis while percentage of the population shown in y-axis. The population range is small in HR $\Delta rolC$ comparing with the other groups. Moreover, branch root number of HR $\Delta rolC$ also decreased drastically. Box plot of each group are shown in (B) where the dots represent the outliers. Significant differences were analyzed using permutation by ANOVA with 1000 replications against HR WT. (** $p < 0.01$, *** $p < 0.001$).

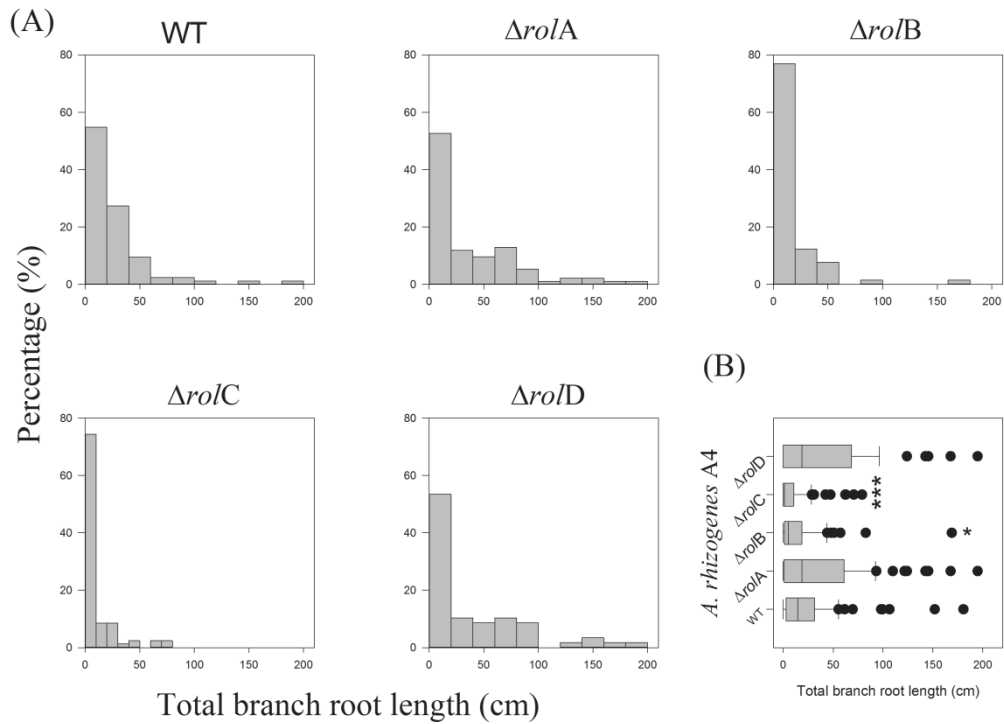


Figure 3-10. Total branch root length of *A. rhizogenes* A4 and its *rol* gene-deficient derivatives.

Population distribution of each groups are shown in (A). Total branch root length is shown in x-axis while percentage of the population shown in y-axis. Box plot of each group are shown in (B) where the dots represent the outliers. Significant differences were analyzed using permutation by ANOVA with 1000 replications against HR WT. (* $p < 0.05$, *** $p < 0.001$).

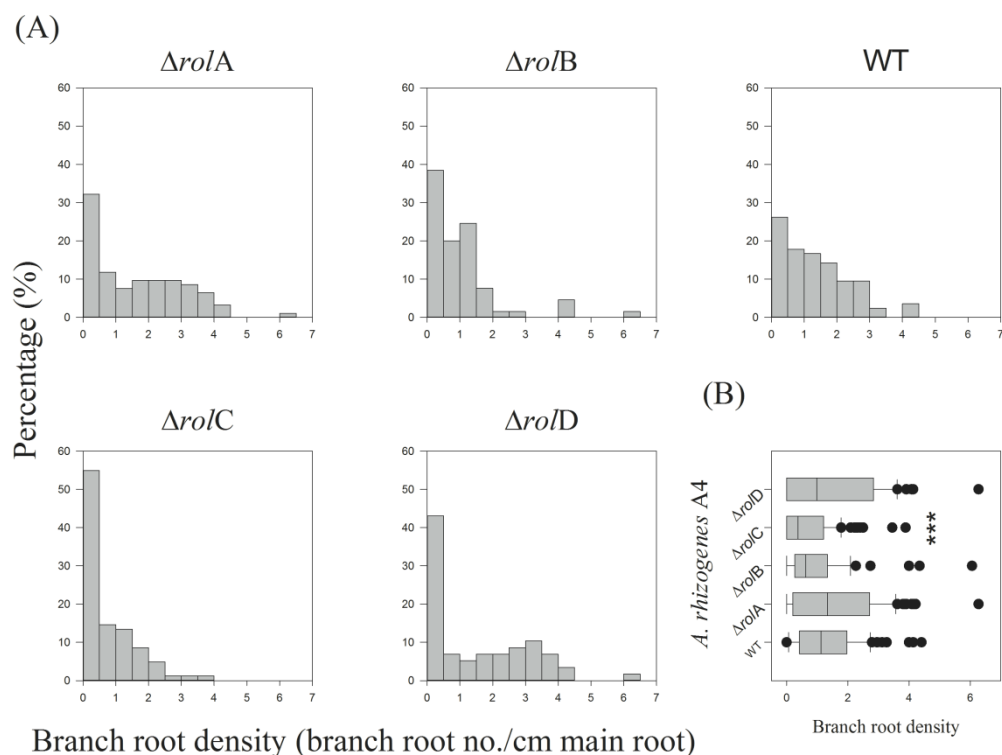


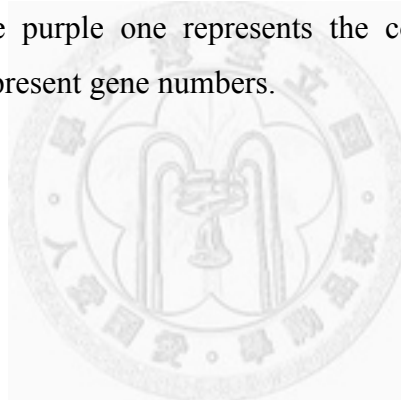
Figure 3-11. Branch root density of *A. rhizogenes* A4 and its *rol* gene-deficient derivatives.

Population distribution of each groups are shown in (A). Total branch root length is shown in x-axis while percentage of the population shown in y-axis. Box plot of each group are shown in (B) where the dots represent the outliers. Significant differences were analyzed using permutation by ANOVA with 1000 replications against HR WT. (***) $p < 0.001$).



Figure 3-12. The constitutive expressed gene under 2-fold cut off.

The red circle represents genes extracted in first biological replicate, the blue circle represents the second. The purple one represents the constitutive expressed genes. Numbers within the area represent gene numbers.



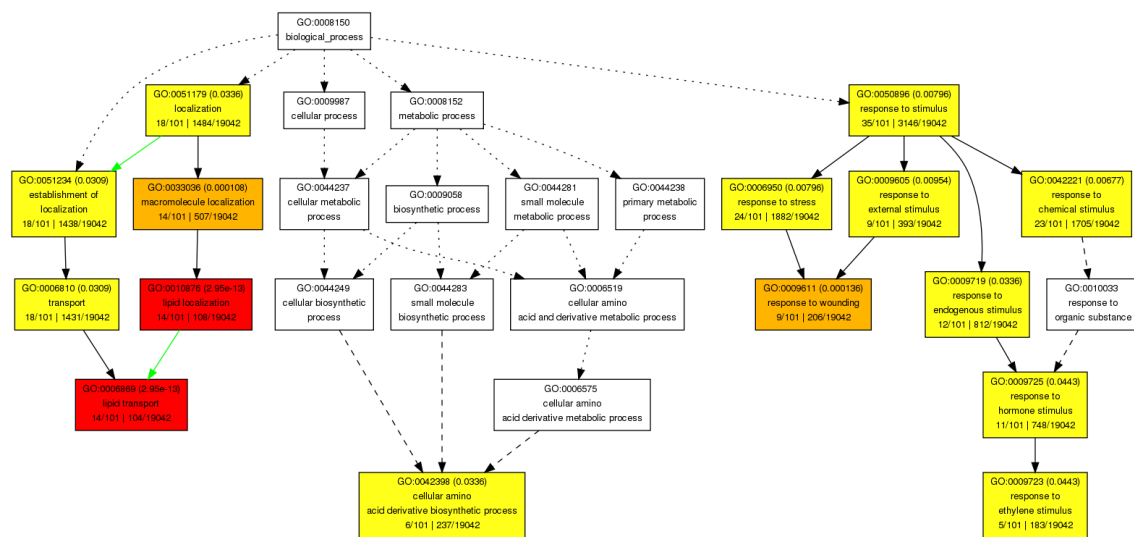


Figure 3-13. Gene ontology of HR $\Delta rolB$ down-regulated genes.

Gene ontology was performed by AgriGO under default conditions (p-value 0.05). Each box represents a gene group according to the molecular function with brief description in the box, where the *p*-value was also shown. The color of the box turns from white to yellow to red when the significant difference increases. Lipid binding was the most enriched group, indicating that lipid binding may be regulated by *rolB*. Hydrolyzing O-glycosyl compounds and peroxidase activity were also affected.

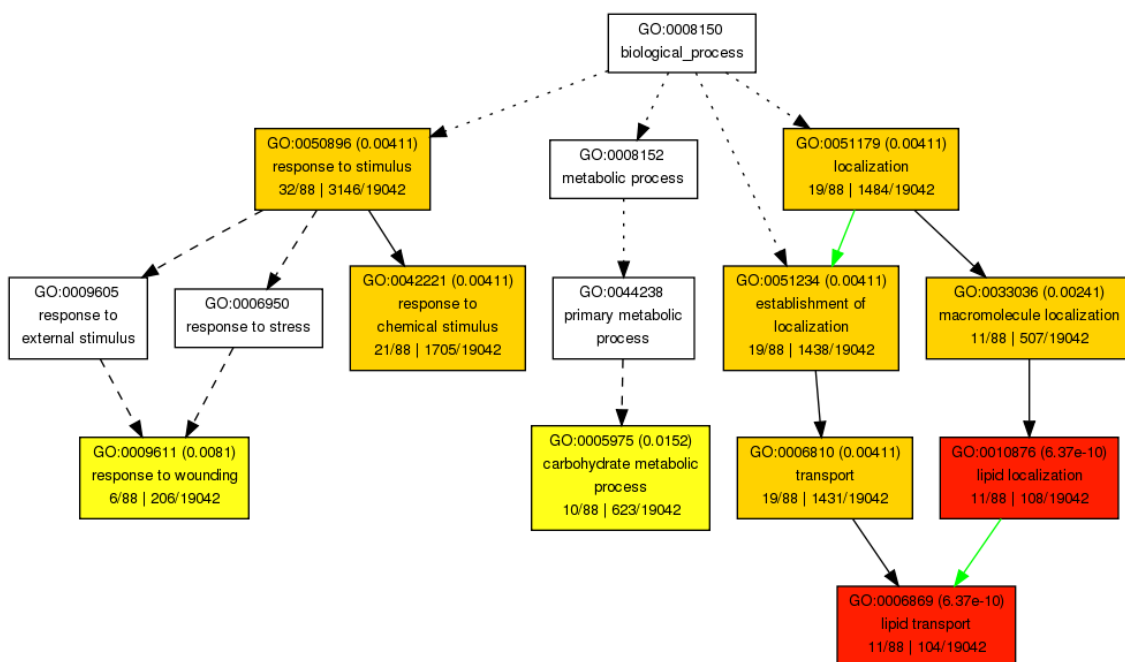


Figure 3-14. Gene ontology of HR $\Delta rolC$ down-regulated genes.

Gene ontology was performed by AgriGO under default conditions (p-value 0.05). Each box represents a gene group according to the molecular function with brief description in the box, where the p-value is also shown. The color of the box turns from white to yellow to red when the significant different increases. Lipid binding was the most drastic affected group. Besides, carbohydrate metabolic process and respond to wounding are also extracted.

References

- Altamura MM, Archilletti T, Capone I, Costantino P** (1991) Histological analysis of the expression of *Agrobacterium rhizogenes* *rolB*-GUS gene fusions in transgenic tobacco. *New Phytol* **118**: 69-78
- Altamura MM, Capitani F, Gazza L, Capone I, Costantino P** (1994) The plant oncogene *rolB* stimulates the formation of flower and root meristemoids in tobacco thin cell-layers. *New Phytol* **126**: 283-293
- Ark PA, Thompson JP** (1961) Detection of hairy root pathogen, *Agrobacterium rhizogenes*, by use of fleshy roots. *Phytopathology* **51**: 69-71
- Armando Aguado-Santacruz G, Rascon-Cruz Q, Moreno-Gomez B, Gerardo Guevara-Gonzalez R, Guevara-Olvera L, Francisco Jimenez-Bremont J, Arevalo-Gallegos S, Garcia-Moya E** (2009) Genetic transformation of blue grama grass with the *rolA* gene from *Agrobacterium rhizogenes*: regeneration of transgenic plants involves a "hairy embryo" stage. *In Vitro Cell Dev-Pl* **45**: 681-692
- Banerjee S, Shang TQ, Wilson AM, Moore AL, Strand SE, Gordon MP, Doty SL** (2002) Expression of functional mammalian P450 2E1 in hairy root cultures. *Biotechnol Bioeng* **77**: 462-466
- Banerjee S, Singh S, Rahman LU** (2012) Biotransformation studies using hairy root cultures — A review. *Biotechnol Adv* **30**: 461-468
- Bariola PA, Howard CJ, Taylor CB, Verbarg MT, Jaglan VD, Green PJ** (1994) The *Arabidopsis* ribonuclease gene *RNS1* is tightly controlled in response to phosphate limitation. *Plant J* **6**: 673-685
- Batra J, Dutta A, Singh D, Kumar S, Sen J** (2004) Growth and terpenoid indole alkaloid production in *Catharanthus roseus* hairy root clones in relation to left- and right-termini-linked Ri T-DNA gene integration. *Plant Cell Rep* **23**: 148-154
- Bonferroni CE** (1936) *Teoria statistica delle classi e calcolo delle probabilit `a*. Pubblicazioni del R Istituto Superiore di Scienze Economiche e Commerciali di Firenze **8**: 3-62
- Bulgakov VP** (2008) Functions of *rol* genes in plant secondary metabolism. *Biotechnol Adv* **26**: 318-324
- Bulgakov VP, Khodakovskaya MV, Labetskaya NV, Chernoded GK, Zhuravlev YN** (1998) The impact of plant *rolC* oncogene on ginsenoside production by ginseng hairy root cultures. *Phytochemistry* **49**: 1929-1934
- Capone I, Cardarelli M, Trovato M, Costantino P** (1989) Upstream non-coding region which confers polar expression to Ri plasmid root inducing gene *rolB*. *Mol Gen Genet* **216**: 239-244

- Capone I, Frugis G, Costantino P, Cardarelli M** (1994) Expression in different populations of cells of the root-meristem is controlled by different domains of the *rolB* promoter. *Plant Mol Biol* **25**: 681-691
- Capone I, Spano L, Cardarelli M, Bellincampi D, Petit A, Costantino P** (1989) Induction and growth properties of carrot roots with different complements of *Agrobacterium rhizogenes* T-DNA. *Plant Mol Biol* **13**: 43-52
- Cardarelli M, Mariotti D, Pomponi M, Spanò L, Capone I, Costantino P** (1987) *Agrobacterium rhizogenes* T-DNA genes capable of inducing hairy root phenotype. *Mol Gen Genet* **209**: 475-480
- Cardarelli M, Spanò L, Mariotti D, Mauro ML, Sluys MA, Costantino P** (1987) The role of auxin in hairy root induction. *Mol Gen Genet* **208**: 457-463
- Carneiro M, Vilaine F** (1993) Differential expression of the *rolA* plant oncogene and its effect on tobacco development. *Plant J* **3**: 785-792
- Chichiricco G, Costantino P, Spano L** (1992) Expression of the *rolB* oncogene from *Agrobacterium rhizogenes* during zygotic embryogenesis in tobacco. *Plant Cell Physiol* **33**: 827-832
- De Smet I, Tetsumura T, De Rybel B, Frey NFd, Laplaze L, Casimiro I, Swarup R, Naudts M, Vanneste S, Audenaert D, Inzé D, Bennett MJ, Beeckman T** (2007) Auxin-dependent regulation of lateral root positioning in the basal meristem of *Arabidopsis*. *Development* **134**: 681-690
- Du Z, Zhou X, Ling Y, Zhang Z, Su Z** (2010) agriGO: a GO analysis toolkit for the agricultural community. *Nucleic acids Res* **38**: W64-70
- Elmayan T, Tepfer M** (1995) Evaluation in tobacco of the organ specificity and strength of the *rolD* promoter, domain A of the 35S promoter and the 35S2 promoter. *Transgenic Res* **4**: 388-396
- Estruch JJ, Chriqui D, Grossmann K, Schell J, Spena A** (1991) The plant oncogene *rolC* is responsible for the release of cytokinins from glucoside conjugates. *Embo J* **10**: 2889-2895
- Estruch JJ, Parets-Soler A, Schmulling T, Spena A** (1991) Cytosolic localization in transgenic plants of the RolC peptide from *Agrobacterium rhizogenes*. *Plant Mol Biol* **17**: 547-550
- Estruch JJ, Schell J, Spena A** (1991) The protein encoded by the *rolB* plant oncogene hydrolyzes indole glucosides. *Embo J* **10**: 3125-3128
- Faiss M, Strnad M, Redig P, Doležal K, Hanuš J, Van Onckelen H, Schmülling T** (1996) Chemically induced expression of the *rolC*-encoded β -glucosidase in transgenic tobacco plants and analysis of cytokinin metabolism: *rolC* does not hydrolyze endogenous cytokinin glucosides in planta. *Plant J* **10**: 33-46
- Falasca G, Altamura MM, D'Angeli S, Zaghi D, Costantino P, Mauro ML** (2010)

- The *rolD* oncogene promotes axillary bud and adventitious root meristems in *Arabidopsis*. *Plant Physiol Biochem* **48**: 797-804
- Filippini F, Loschiavo F, Terzi M, Costantino P, Trovato M** (1994) The plant oncogene *rolB* alters binding of auxin to plant-cell membranes. *Plant Cell Physiol* **35**: 767-771
- Filippini F, Rossi V, Marin O, Trovato M, Costantino P, Mark Downey P, Lo Schiavo F, Terzi M** (1996) A plant oncogene as a phosphatase. *Nature* **379**: 499-500
- Friml J, Wisniewska J, Benkova E, Mendgen K, Palme K** (2002) Lateral relocation of auxin efflux regulator PIN3 mediates tropism in *Arabidopsis*. *Nature* **415**: 806-809
- Fujii N** (1997) Pattern of DNA binding of nuclear proteins to the proximal *Agrobacterium rhizogenes* *rolC* promoter is altered during somatic embryogenesis of carrot. *Gene* **201**: 55-62
- Furmanowa M, Syklowska-Baranek K** (2000) Hairy root cultures of *Taxus* × media var. *Hicksii* Rehd. as a new source of paclitaxel and 10-deacetylbaccatin III. *Biotechnol Lett* **22**: 683-686
- García-Olmedo F, Molina A, Segura A, Moreno M** (1995) The defensive role of nonspecific lipid-transfer proteins in plants. *Trends Microbiol* **3**: 72-74
- Gaume A, Komarnytsky S, Borisjuk N, Raskin I** (2003) Rhizosecretion of recombinant proteins from plant hairy roots. *Plant Cell Rep* **21**: 1188-1193
- Guivarch A, Carneiro M, Vilaine F, Pautot V, Chriqui D** (1996) Tissue-specific expression of the *rolA* gene mediates morphological changes in transgenic tobacco. *Plant Mol Biol* **30**: 125-134
- Hamill JD, Parr AJ, Robins RJ, Rhodes MJC** (1986) Secondary product formation by cultures of *Beta vulgaris* and *Nicotiana rustica* transformed with *Agrobacterium rhizogenes*. *Plant Cell Rep* **5**: 111-114
- Hamilton AJ, Lycett GW, Grierson D** (1990) Antisense gene that inhibits synthesis of the hormone ethylene in transgenic plants. *Nature* **346**: 284-287
- Hernández-Mata G, Mellado-Rojas M, Richards-Lewis A, López-Bucio J, Beltrán-Peña E, Soriano-Bello E** (2010) Plant immunity induced by oligogalacturonides alters root growth in a process involving flavonoid accumulation in *Arabidopsis thaliana*. *J Plant Growth Regul* **29**: 441-454
- Huffman GA, White FF, Gordon MP, Nester EW** (1984) Hairy-root-inducing plasmid: physical map and homology to tumor-inducing plasmids. *J Bacteriol* **157**: 269-276
- Jayaraj J, Devlin R, Punja Z** (2008) Metabolic engineering of novel ketocarotenoid production in carrot plants. *Transgenic Res* **17**: 489-501

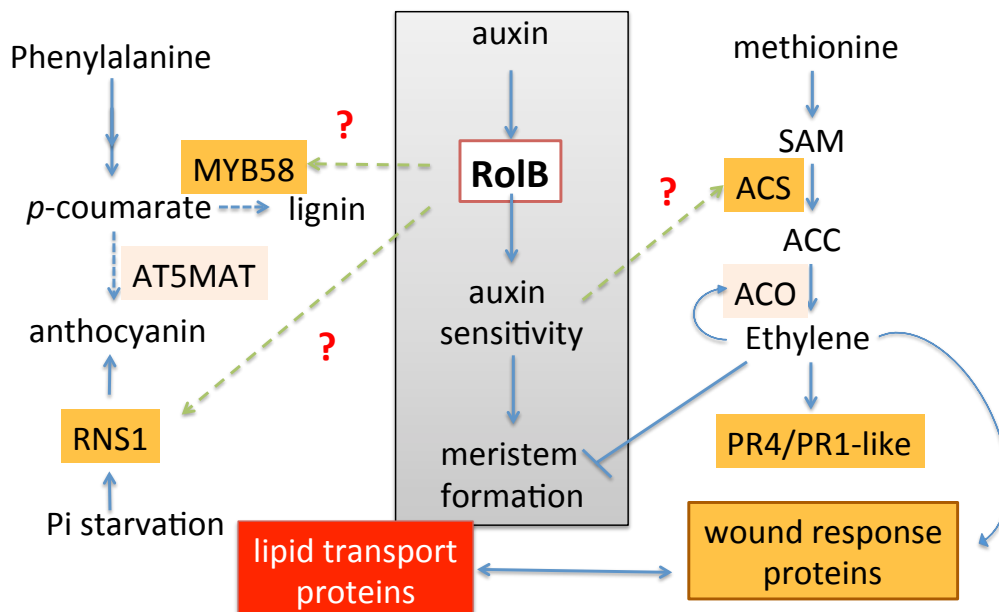
- Jung HW, Kim W, Hwang BK** (2003) Three pathogen-inducible genes encoding lipid transfer protein from pepper are differentially activated by pathogens, abiotic, and environmental stresses. *Plant, Cell Environ* **26**: 915-928
- Kamo KK** (2003) Long-term expression of the *uidA* gene in gladiolus plants under control of either the ubiquitin, rolD, mannopine synthase, or cauliflower mosaic virus promoters following three seasons of dormancy. *Plant Cell Rep* **21**: 797-803
- Kim JA, Baek KH, Son YM, Son SH, Shin H** (2009) Hairy root cultures of *Taxus cuspidata* for enhanced production of paclitaxel. *J Korean Soc Appl Biol Chem* **52**: 144-150
- Kiselev KV, Dubrovina AS, Bulgakov VP** (2009) Phenylalanine ammonia-lyase and stilbene synthase gene expression in rolB transgenic cell cultures of *Vitis amurensis*. *Appl Microbiol Biotechnol* **82**: 647-655
- Kiselev KV, Dubrovina AS, Veselova MV, Bulgakov VP, Fedoreyev SA, Zhuravlev YN** (2007) The *rolB* gene-induced overproduction of resveratrol in *Vitis amurensis* transformed cells. *J Biotechnol* **128**: 681-692
- Kruskal WH** (1957) Historical notes on the Wilcoxon unpaired two-sample test. *J Am Stat Assoc* **52**: 356-360
- Kruskal WH, Wallis WA** (1952) Use of ranks in one-criterion variance analysis. *J Am Stat Assoc* **47**: 583-621
- Leach F, Aoyagi K** (1991) Promoter analysis of the highly expressed *rolC* and *rolD* root-inducing genes of *Agrobacterium rhizogenes*: enhancer and tissue-specific DNA determinants are dissociated. *Plant Sci* **79**: 69-76
- Lee KT, Chen SC, Chiang BL, Yamakawa T** (2007) Heat-inducible production of beta-glucuronidase in tobacco hairy root cultures. *Appl Microbiol Biotechnol* **73**: 1047-1053
- Levesque H, Delepelaire P, Rouzé P, Slightom J, Tepfer D** (1988) Common evolutionary origin of the central portions of the Ri TL-DNA of *Agrobacterium rhizogenes* and the Ti T-DNAs of *Agrobacterium tumefaciens*. *Plant Mol Biol* **11**: 731-744
- Lewis DR, Negi S, Sukumar P, Muday GK** (2011) Ethylene inhibits lateral root development, increases IAA transport and expression of PIN3 and PIN7 auxin efflux carriers. *Development* **138**: 3485-3495
- Magrelli A, Langenkemper K, Dehio C, Schell J, Spena A** (1994) Splicing of the *rolA* transcript of *Agrobacterium rhizogenes* in *Arabidopsis*. *Science* **266**: 1986-1988
- Matsuki R, Uchimiya H** (1994) A 43-kDa nuclear tobacco protein interacts with a specific single-stranded DNA sequence from the 5'-upstream region of the

- Agrobacterium rhizogenes rolC* gene. *Gene* **141**: 201-205
- Maurel C, Brevet J, Barbierbrygoo H, Guern J, Tempe J** (1990) Auxin regulates the promoter of the root-inducing *rolB* gene of *Agrobacterium rhizogenes* in transgenic tobacco. *Mol Gen Genet* **223**: 58-64
- Mauro ML, Trovato M, Paolis AD, Gallelli A, Costantino P, Altamura MM** (1996) The plant oncogene *rolD* stimulates flowering in transgenic tobacco plants. *Dev Biol* **180**: 693-700
- McInnes E, Morgan AJ, Mulligan BJ, Davey MR** (1991) Phenotypic effects of isolated pRiA4 TL-DNA *rol* genes in the presence of intact TR-DNA in transgenic plants of *Solanum dulcamara* L. *J Exp Bot* **42**: 1279-1286
- Negi S, Ivanchenko MG, Muday GK** (2008) Ethylene regulates lateral root formation and auxin transport in *Arabidopsis thaliana*. *Plant J* **55**: 175-187
- Nilsson O, Crozier A, Schmülling T, Sandberg G, Olsson O** (1993) Indole-3-acetic acid homeostasis in transgenic tobacco plants expressing the *Agrobacterium rhizogenes rolB* gene. *Plant J* **3**: 681-689
- Nilsson O, Moritz T, Imbault N, Sandberg G, Olsson O** (1993) Hormonal characterization of transgenic tobacco plants expressing the *rolC* Gene of *Agrobacterium rhizogenes* TL-DNA. *Plant Physiol* **102**: 363-371
- O'Donnell PJ, Calvert C, Atzorn R, Wasternack C, Leyser HMO, Bowles DJ** (1996) Ethylene as a Signal Mediating the Wound Response of Tomato Plants. *Science* **274**: 1914-1917
- Ono NN, Tian L** (2011) The multiplicity of hairy root cultures: Prolific possibilities. *Plant Sci* **180**: 439-446
- Ooms G, Twell D, Bossen ME, Hoge JHC, Burrell MM** (1986) Developmental regulation of Ri TL-DNA gene expression in roots, shoots and tubers of transformed potato (*Solanum tuberosum* cv. Desiree). *Plant Mol Biol* **6**: 321-330
- Oono Y, Satomi T, Uchimiya H** (1991) *Agrobacterium rhizogenes* LacZ-*rolC* gene expression in *Escherichia coli* - detection of the product in transgenic plants using RolC-specific antibodies. *Gene* **104**: 95-98
- Rigden DJ, Carneiro M** (1999) A structural model for the *rolA* protein and its interaction with DNA. *Proteins: Struct, Funct, Bioinf* **37**: 697-708
- Riker AJ, Banfield WM, Wright WH, Keitt GW, Sagen HE** (1930) Studies on infectious hairy root of nursery apple trees. *J Agric Res* **41**: 0507-0540
- Schmülling T, Fladung M, Grossmann K, Schell J** (1993) Hormonal content and sensitivity of transgenic tobacco and potato plants expressing single *rol* genes of *Agrobacterium rhizogenes* T-DNA. *Plant J* **3**: 371-382
- Schmullling T, Schell J, Spena A** (1988) Single genes from *Agrobacterium rhizogenes* influence plant development. *Embo J*. **7**: 2621-2629

- Schmullig T, Schell J, Spena A** (1989) Promoters of the *rolA*, *B*, and *C* genes of *Agrobacterium rhizogenes* are differentially regulated in transgenic plants. *Plant Cell* **1**: 665-670
- Slightom JL, Durand-Tardif M, Jouanin L, Tepfer D** (1986) Nucleotide sequence analysis of TL-DNA of *Agrobacterium rhizogenes* agropine type plasmid. Identification of open reading frames. *J Biol Chem* **261**: 108-121
- Slightom JL, Jouanin L, Leach F, Drong RF, Tepfer D** (1985) Isolation and identification of TL-DNA/plant junctions in *Convolvulus arvensis* transformed by *Agrobacterium rhizogenes* strain A4. *Embo J*. **4**: 3069-3077
- Spano L, Wullems GJ, Schilperoort RA, Costantino P** (1981) Hairy root - *in vitro* growth properties of tissues induced by *Agrobacterium rhizogenes* on tobacco. *Plant Sci Lett* **23**: 299-305
- Spena A, Estruch JJ, Prinsen E, Nacken W, Vanonckelen H, Sommer H** (1992) Anther-specific expression of the *rolB* Gene of *Agrobacterium rhizogenes* increases IAA content in anthers and alters anther development and whole flower growth. *Theor Appl Genet* **84**: 520-527
- Sugaya S, Hayakawa K, Handa T, Uchimiya H** (1989) Cell-specific expression of the *rolC* gene of the TL-DNA of Ri plasmid in transgenic tobacco plants. *Plant Cell Physiol* **3**: 649-654
- Sugaya S, Uchimiya H** (1992) Deletion analysis of the 5'-upstream region of the *Agrobacterium rhizogenes* Ri plasmid *rolC* gene required for tissue-specific expression. *Plant Physiol* **99**: 464-467
- Sun L-Y, Monneuse M-O, Martin-Tanguy J, Tepfer D** (1991) Changes in flowering and the accumulation of polyamines and hydroxycinnamic acid-polyamine conjugates in tobacco plants transformed by the *rolA* locus from the Ri TL-DNA of *Agrobacterium rhizogenes*. *Plant Sci* **80**: 145-156
- Suzuki A, Kato A, Uchimiya H** (1992) Single-stranded DNA of 5'-upstream region of the *rolC* gene interacts with nuclear proteins of carrot cell cultures. *Biochem Biophys Res Commun* **188**: 727-733
- Swain SS, Sahu L, Barik DP, Chand PK** (2010) *Agrobacterium* × plant factors influencing transformation of 'Joseph's coat' (*Amaranthus tricolor* L.). *Sci Hortic-Amsterdam* **125**: 461-468
- Tamot BK, Pauls KP, Glick BR** (2003) Root and hypocotyl growth in transgenic tomatoes that express the bacterial enzyme ACC deaminase. *J Plant Biol* **46**: 181-186
- Taylor BH, White FF, Nester EW, Gordon MP** (1985) Transcription of *Agrobacterium rhizogenes* A4 T-DNA. *Mol Gen Genet* **201**: 546-553
- Team RDC** (2011) R: A language and environment for statistical computing.

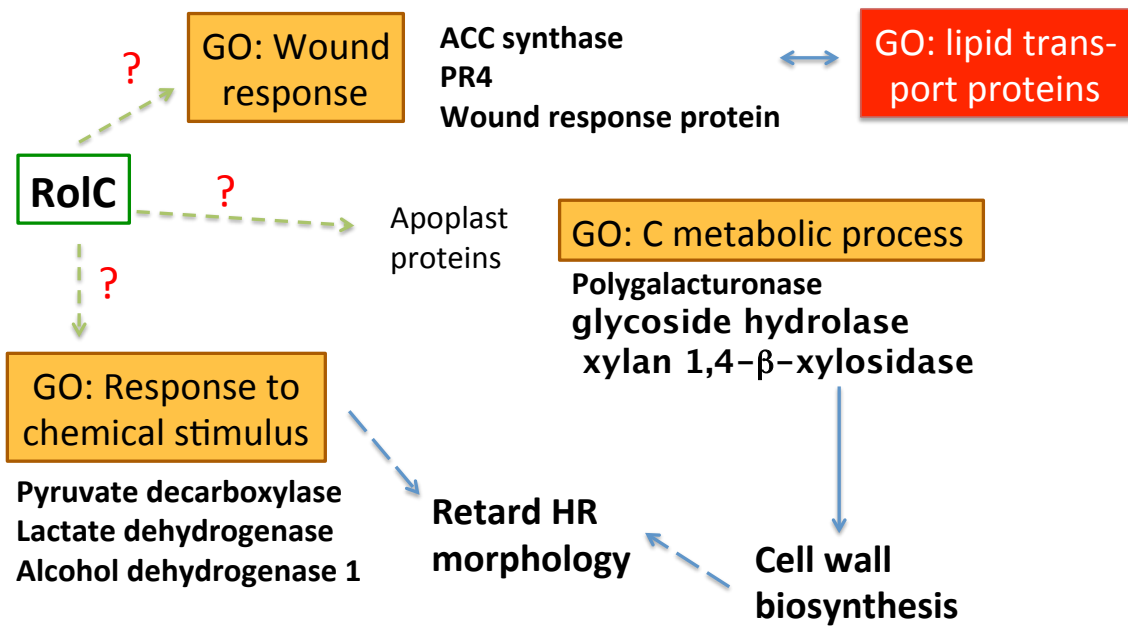
- Toivonen L** (1993) Utilization of hairy root cultures for production of secondary metabolites. *Biotechnol Prog* **9**: 12-20
- Trovato M, Maras B, Linhares F, Costantino P** (2001) The plant oncogene *rolD* encodes a functional ornithine cyclodeaminase. *Proc Natl Acad Sci USA* **98**: 13449-13453
- Van Altvorst AC, Bino RJ, Van Dijk AJ, Lamers AMJ, Lindhout WH, Van Der Mark F, Dons JJM** (1992) Effects of the introduction of *Agrobacterium rhizogenes* *rol* genes on tomato plant and flower development. *Plant Sci (Shannon)* **83**: 77-85
- Vilaine F, Cassedelbart F** (1987) Independent induction of transformed roots by the TL and TR regions of the Ri plasmid of agropine type *Agrobacterium rhizogenes*. *Mol Gen Genet* **206**: 17-23
- Vilaine F, Cassedelbart F** (1987) A new vector derived from *Agrobacterium rhizogenes* plasmids: a micro-Ri plasmid and its use to construct a mini-Ri plasmid. *Gene* **55**: 105-114
- Vilaine F, Rembur J, Chriqui D, Tepfer M** (1998) Modified development in transgenic tobacco plants expressing a *rolA::GUS* translational fusion and subcellular localization of the fusion protein. *Mol Plant Microbe In* **11**: 855-859
- Welander M, Zhu L-H** (2010) Rol Genes: Molecular Biology, Physiology, Morphology, Breeding Uses. *In Plant Breeding Reviews*. John Wiley & Sons, Inc., pp 79-103
- White FF, Ghidossi G, Gordon MP, Nester EW** (1982) Tumor induction by *Agrobacterium rhizogenes* involves the transfer of plasmid DNA to the plant genome. *Proc Natl Acad Sci USA* **79**: 3193-3197
- White FF, Nester EW** (1980) Hairy root: plasmid encodes virulence traits in *Agrobacterium rhizogenes*. *J Bacteriol* **141**: 1134-1141
- White FF, Taylor BH, Huffman GA, Gordon MP, Nester EW** (1985) Molecular and genetic analysis of the transferred DNA regions of the root-inducing plasmid of *Agrobacterium rhizogenes*. *J Bacteriol* **164**: 33-44
- Xue Z-T, Holfors A, Welander M** (2008) Intron splicing in 5' untranslated region of the *rolA* transcript in transgenic apple. *J Plant Physiol* **165**: 544-552
- Yokoyama R, Hirose T, Fujii N, Aspuria ET, Kato A, Uchimiya H** (1994) The *rolC* promoter of *Agrobacterium rhizogenes* Ri plasmid is activated by sucrose in transgenic tobacco plants. *Mol Gen Genet* **244**: 15-22
- Zhou J, Lee C, Zhong R, Ye Z-H** (2009) MYB58 and MYB63 Are Transcriptional Activators of the Lignin Biosynthetic Pathway during Secondary Cell Wall Formation in Arabidopsis. *Plant Cell* **21**: 248-266

Appendix



Appendix 1. Biological functions of *rolB*.

Gray background represent previous knowledge about *RolB*: *RolB* is known to be induced by auxin and were able to increase the auxin sensitivity of the plant cell, which lead to meristem formation. Yellow and red blocks represent genes extracted from gene ontology. *RolB* may regulate ethylene biosynthesis and / or response in an unknown mechanism. Lipid transport may be regulated through the wound response proteins. On the other hand, it may regulate lignin biosynthesis through MYB58. It may also regulate the biosynthesis of anthocyanin, a plant secondary metabolite, through ribonuclease 1 (*RNS1*).



Appendix 2. Biological functions of *rolC*.

RolC may interact with the wound response proteins through an unknown mechanism. These wound response proteins may then regulate the lipid transport proteins. On the other hand, *RolC* may also regulate the carbohydrate metabolic process proteins that result in impair cell wall biosynthesis, which lead to retard HR $\Delta rolC$ morphology observed in this study. Meanwhile, *RolC* may also regulate the response to chemical stimulus protein that is directly related to carbon metabolism and lead to the retard morphology of HR $\Delta rolC$. Yellow and red blocks represent genes extracted from gene ontology.